Mon. Not. R. Astron. Soc. **281,** 425–448 (1996)

Optical spectroscopy and polarization of a new sample of optically bright flat radio spectrum sources

M. J. M. Marchã,[1] I. W. A. Browne,[2] C. D. Impey[3] and P. S. Smith[3]

[1]*DICE Universidade de Lisboa, Av. Prof. Gama Pinto, 2, 1699 Lisboa Codex, Portugal*
[2]*NRAL Jodrell Bank, University of Manchester, Macclesfield, Cheshire SK11 9DL*
[3]*Steward Observatory, University of Arizona, Tucson, AZ 85721, USA*

Accepted 1995 December 21. Received 1995 December 19; in original form 1995 July 6

ABSTRACT

A new sample of bright flat radio spectrum sources selected at 8.4 GHz and consisting of objects brighter than $V=17$ is discussed. The sample was selected with three purposes in mind: (i) to find low-luminosity BL Lacertae (BL Lac) objects with radio luminosities comparable to those of BL Lacs selected at X-ray frequencies; (ii) to investigate the differences between BL Lacs and other flat radio spectrum sources; and (iii) to define a sample of nearby radio-loud objects, the host galaxies of which are easy to study. Using information on four observational parameters, radio polarization, optical percentage polarization, break contrast and equivalent width of the strongest emission line, we compare the properties of BL Lacs with those of other types of active galactic nuclei (AGN) found in the sample. We find that most of the objects have weak emission lines although some sources with Seyfert-type spectra were also found. With only a few exceptions, the two types of sources appear well separated in their observational properties. Among the objects studied we report 10 new BL Lacs and BL Lac candidates, and we define a 'complete' sample of bright flat radio spectrum sources that consists of those objects with redshift ≤ 0.1.

Key words: polarization – BL Lacertae objects: general – galaxies: nuclei – radio continuum: general.

1 INTRODUCTION

BL Lacertae (BL Lac) objects are active galactic nuclei (AGN) which display rapid optical variability, high and variable optical polarization and weak or non-existent emission lines. These properties indicate that a large part of the optical continuum emission is non-thermal and it is widely believed that it is relativistically beamed emission originating from nuclear jets (Blandford & Rees 1978). All BL Lac objects are radio-loud (Angel & Stockman 1980; Stocke et al. 1990). Samples of BL Lacs are obtained from either radio or X-ray surveys but, in both cases, optical follow-up observations to measure polarization, variability, strength of emission lines, etc., are required to separate out the BL Lac objects from the vast majority of other AGN in the surveys. The criteria used to define BL Lac objects have been mostly determined by practical observing considerations rather than real physical distinctions between different types of objects. For example, for an object to be classified as a BL Lac, it is common to require the percentage polarization of the optical continuum emission to be larger than 2 or 3 per cent in order to distinguish intrinsic synchrotron polarization from the low, but ubiquitous, polarization imprinted by interstellar dust grains in our own Galaxy (Impey & Tapia 1990). An alternative criterion is that there should be enough extra continuum present in addition to the starlight of the host galaxy to reduce the observed 'contrast' either side of the 4000-Å break to ≤ 0.25 (Stocke et al. 1991). Both of these definitions suffer from the problem that the strength of the non-thermal continuum is being measured relative to that of the host galaxy starlight, something which may have little relation to the properties of the active nucleus. Similarly, the common requirement that the equivalent width (EW) of the strongest emission line be less than 5 Å (Stickel et al. 1991; Stocke et al. 1991) is a very indirect indicator of the presence of non-thermal core emission – one that is both redshift- and luminosity-dependent.

In the face of these difficulties there are two approaches

that one can take to define BL Lac samples. The first is to quantify the effect of the arbitrary selection criteria so that, when comparisons between the statistical properties of different samples are made, it is clear what arises from intrinsic differences and what is simply produced by the effects of different selection criteria. We have done this in a series of papers (Browne & Marchã 1993; Marchã & Browne 1995, 1996). The other approach, which we adopt here, is to take a complete sample of AGN which contains a mixture of BL Lacs and other objects and make detailed measurements of their properties. By not imposing strict selection criteria for the classification of a source as a BL Lac, we hope to investigate any 'natural' breaks in the distribution of observational parameters in the entire sample. The main goal is to see if there are limits to the visibility of the BL Lac phenomenon, or if extremely low-luminosity non-thermal cores can be detected.

Another interest we have is to find radio-selected BL Lacs (RBLs) with radio luminosities more directly comparable to those of BL Lacs found in X-ray surveys (XBLs), in particular those of the *Einstein* Extended Medium Sensitivity Survey 'complete' sample (EMSS-C) (Morris et al. 1991). We have selected a sample of relatively weak flat radio spectrum sources at low redshift so that we can compare radio- and X-ray-selected BL Lacs at similar radio luminosities. The paper is organized as follows. In Sections 2 and 3 we introduce the 200-mJy sample and describe the optical observations, both spectroscopy and polarimetry. The results of the observations are given in Section 4 and in Section 5 we discuss those results. Finally in Section 6 we summarize and present the conclusions.

2 THE SAMPLE

The sample we have chosen to study has been selected from the catalogue of ~ 1500 flat radio spectrum core-dominated sources (Patnaik et al. 1992; A. Patnaik, private communication). The radio observations for this survey were carried out at 8.4 GHz at the Very Large Array (VLA) in its A-configuration and the resulting maps have a resolution of 200 mas (Patnaik et al. 1992). The sources were initially selected from the Green Bank surveys at 1.5 and 5 GHz by Condon & Broderick (1985, 1986) and Condon, Broderick & Seieslad (1989). The following selection criteria were adopted:

(i) $\delta \geq 20°$ and $|b| \geq 12°$;
(ii) $S_{5\,\mathrm{GHz}} \geq 200$ mJy;
(iii) $z \leq 0.2$ if the object had a known redshift;
(iv) $\alpha_r \leq 0.5$ (typically in the range 1 to 5 GHz, and $S_\nu \sim \nu^{-\alpha}$);
(v) the optical identification made from the Palomar Observatory Sky Survey (POSS) satisfied the following:
(a) $V \leq 17$ if the identification was either a galaxy (G), or a red stellar object (RSO), i.e., an object that appeared brighter on the red POSS plate;
(b) $V \leq 16.5$ if the object was either a blue stellar object (BSO), i.e., an object that appeared stellar and brighter on the blue POSS plate, or a neutral stellar object (NSO), an object that appeared equally bright on both POSS plates.

The above selection criteria were adopted for the following reasons. A limit on the galactic latitude ($|b|$) of the objects was imposed in order to avoid problems with galactic extinction. The flux density limit of the Patnaik catalogue is 200 mJy. This limit is five times lower than that of the 1-Jy sample of RBLs (Stickel et al. 1991) which, together with the low-redshift restriction, should ensure the selection of less luminous objects than in the 1-Jy sample, or even in the incomplete S5 sample (Kühr & Schmidt 1990). The third criterion rejects distant objects, again because we want to concentrate on low-luminosity targets. The fourth selects the sources with flat radio spectra. Finally, the fifth criterion selects only bright objects. We aimed to make the survey complete out to a redshift of 0.1 and, since the Hubble diagram for radio galaxies (Smith & Spinrad 1980) shows that only a very small percentage of objects (≤ 5 per cent) fainter than $V = 17$ have redshifts in excess of 0.1, this limiting magnitude for galaxies ensures completeness. The reason for giving a slightly brighter limit to objects that appear stellar on the POSS plates is that their stellar appearance arises from an additional nuclear component which also contributes to the optical flux. This means that for a given optical magnitude they will be at a higher redshift than 'fuzzy' objects the emissions of which are dominated by starlight.

Table 1 lists 57 objects with their B1950 names, their radio positions (J2000) and the optical identification classified according to the appearance on the POSS plates. However, objects previously known to be BL Lacs are listed as such regardless of their appearance. Note that among the 57 objects there are two objects marked with an asterisk, $0149+710$ and $0210+515$, that do not satisfy the galactic latitude selection criterion but were nevertheless observed in the course of this project and were found to be interesting objects.

3 OBSERVATIONS AND ANALYSIS

3.1 Optical spectroscopy

Optical spectroscopy of the 200-mJy sample was obtained at the Multiple Mirror Telescope on Mt Hopkins, on the nights of 1992 May 8–9 and November 2–3. Observations were made with the Red Channel spectrograph, using a 1200×800 Loral CCD detector (Schmidt, Weynmann & Foltz 1989). The CCD has a quantum efficiency of 80 per cent over the wavelength range covered, and a read noise of 6 e^-, which means that all of the spectroscopy is sky-noise limited. A 150 line mm^{-1} grating was used with a UV-36 order blocking filter to give full coverage from [O II] λ3727 Å to [S II] $\lambda\lambda$6716, 6731 Å for the redshifts typical of the 200-mJy sources. Observations through a 1.5-arcsec slit gave a resolution of 20 Å at the blaze wavelength of 4800 Å. Exposures were between 600 and 1200 s for all sources.

The two-dimensional data were reduced according to standard procedures using subroutines in the IRAF package. Wavelength calibration was carried out using helium–neon–argon lamps taken before each exposure; the rms error in the wavelength solution was less than 0.2 resolution elements in all cases (corresponding to 240 km s^{-1}). Flat-fields were applied using an internal quartz lamp after every exposure, in order to minimize the effects of fringing in the

Table 1. The sources of the 200-mJy sample: Name (B1950), RA (J2000), Dec. (J2000) and ID of the 55 objects in the 200-mJy sample. There are two extra objects marked by an asterisk which are not part of the sample but which were also observed (see text for details).

Name (B1950)	RA (J2000.0)	Dec (J2000.0)	ID
0035+227	$00^h\ 38^m\ 08^s.10236$	+23° 03' 28".4396	G
0046+316	00 48 47.14375	+31 57 25.0939	G
0055+300(NGC315)	00 57 48.8868	+30 21 08.8388	G
0109+224	01 12 05.8213	+22 44 38.8020	BL
0116+319(4C31.04)	01 19 34.9991	+32 10 50.0129	G
0125+487	01 28 08.06468	+49 01 05.9766	G
0149+710(*)	01 53 25.85172	+71 15 06.4758	G
0210+515(*)	02 14 17.93188	+51 44 51.9674	G
0251+393	02 54 42.63160	+39 31 34.7140	BSO
0309+411	03 13 01.96146	+41 20 01.1903	G
0316+41(3C84)	03 19 48.16050	+41 30 42.1030	
0321+340	03 24 41.16056	+34 10 45.8053	BSO(w/fuzz)
0651+410	06 55 10.02429	+41 00 10.1479	G
0651+428	06 54 43.52629	+42 47 58.7276	G
0716+714	07 21 53.44880	+71 20 36.3630	BL
0729+562	07 33 28.61493	+56 05 41.7344	G
0733+597	07 37 30.08713	+59 41 03.1948	G
0806+350	08 09 38.88712	+34 55 37.2563	G
0848+686	08 53 18.89863	+68 28 19.0085	G
0902+468	09 06 15.53935	+46 36 19.0197	G
0912+297	09 15 52.40015	+29 33 23.9790	BL
1055+567	10 58 37.72617	+56 28 11.1834	RSO
1101+384(Mrk421)	11 04 27.31462	+38 12 31.7875	BL
1123+203	11 25 58.74395	+20 05 54.3812	G(blue)
1133+704(Mrk180)	11 36 26.40689	+70 09 27.3043	BL
1144+352	11 47 22.13022	+35 01 07.5258	G
1146+596(NGC3894)	11 48 50.35909	+59 24 56.3620	G(E4)
1147+245	11 50 19.21378	+24 17 53.8565	BL
1215+303(ON235)	12 17 52.08378	+30 07 00.6230	BL
1217+295(NGC4278)	12 20 06.82432	+29 16 50.7159	G(E)
1219+285(WCom,ON231)	12 21 31.69080	+28 13 58.4965	BL
1241+735	12 43 11.21561	+73 15 59.2589	G
1245+676	12 47 33.32999	+67 23 16.4568	G
1254+571(Mrk231)	12 56 14.23440	+56 52 25.2367	G
1404+286(OQ208)	14 07 00.39471	+28 27 14.6909	G
1418+546(OQ530)	14 19 46.59750	+54 23 14.7870	BL
1421+511	14 23 14.18676	+50 55 37.2879	G
1424+240	14 27 00.39510	+23 48 00.0410	BL
1532+236(Arp220)	15 34 57.22396	+23 30 11.6084	G
1551+239	15 53 43.59555	+23 48 25.4804	G
1558+595	15 59 01.70269	+59 24 21.8467	G
1645+292	16 47 26.88289	+29 09 49.6025	G
1646+499	16 47 34.91239	+49 50 00.5825	G
1652+398(Mrk501)	16 53 52.21705	+39 45 36.6111	BL
1658+302	17 00 45.22922	+30 08 12.9003	G
1703+223	17 05 29.32990	+22 16 07.5858	G(E)
1744+260	17 46 48.28271	+26 03 20.3475	G
1755+626(NGC6521)	17 55 48.43973	+62 36 44.1193	G
1807+698	18 06 50.68070	+69 49 28.1100	BL
1959+650	19 59 59.85227	+65 08 54.6683	BL
2116+81	21 14 01.17936	+82 04 48.3481	BSO
2202+363	22 04 21.09972	+36 32 37.0944	G
2214+201	22 17 15.84518	+20 24 48.9605	RSO
2217+259	22 19 49.74258	+26 13 27.9589	red,extended obj.
2319+317	23 21 54.95580	+32 04 07.5894	RSO
2320+203	23 23 20.34285	+20 35 23.5182	G
2337+268(NGC7728)	23 40 00.83885	+27 08 01.3728	G(blue)

red part of the spectrum. The spectrograph slit was aligned to the parallactic angle before each exposure to minimize blue light losses. Spectrophotometric standards were observed on each of the four nights. Following bias subtraction, flat-fielding and wavelength calibration, the spectra were extracted using an algorithm that optimizes the signal-to-noise (S/N) ratio in the extended image. Sky subtraction was carried out using a low-order model to the variation in sky level along the slit. Following the derivation of a sensitivity function from standard observations, the spectra were flux calibrated. The spectra are shown in Fig. 1.

3.2 Optical polarimetry

Broad-band, optical linear polarimetry of the 200-mJy sample was acquired using the 90-inch and 61-inch telescopes of Steward Observatory between 1992 April and 1993 April. The optical polarimetry is listed in Tables 2 and 3.

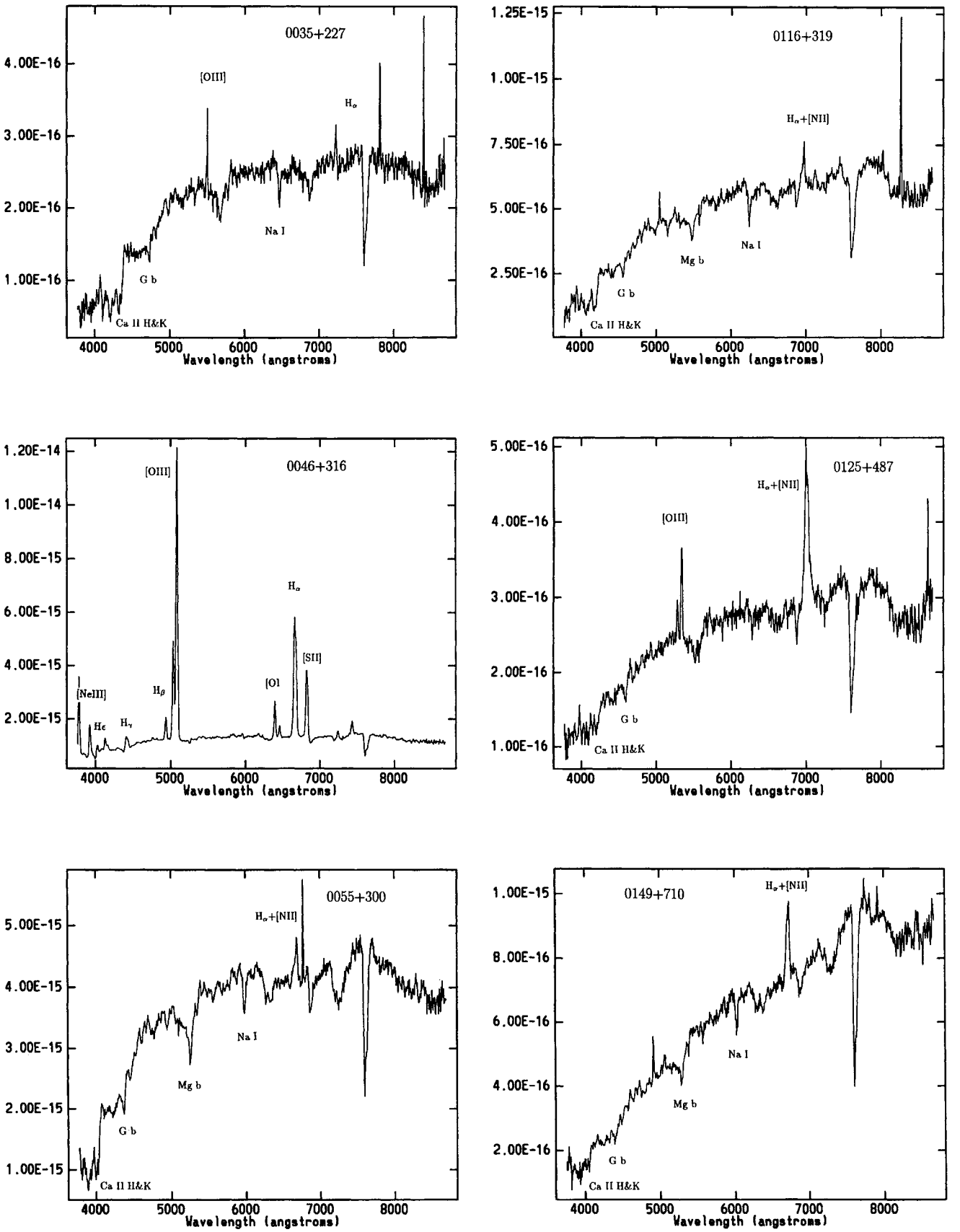

Figure 1. Spectra of the sources in the 200-mJy sample. The spectra are flux calibrated with flux units in erg s^{-1} cm^{-2} $Å^{-1}$.

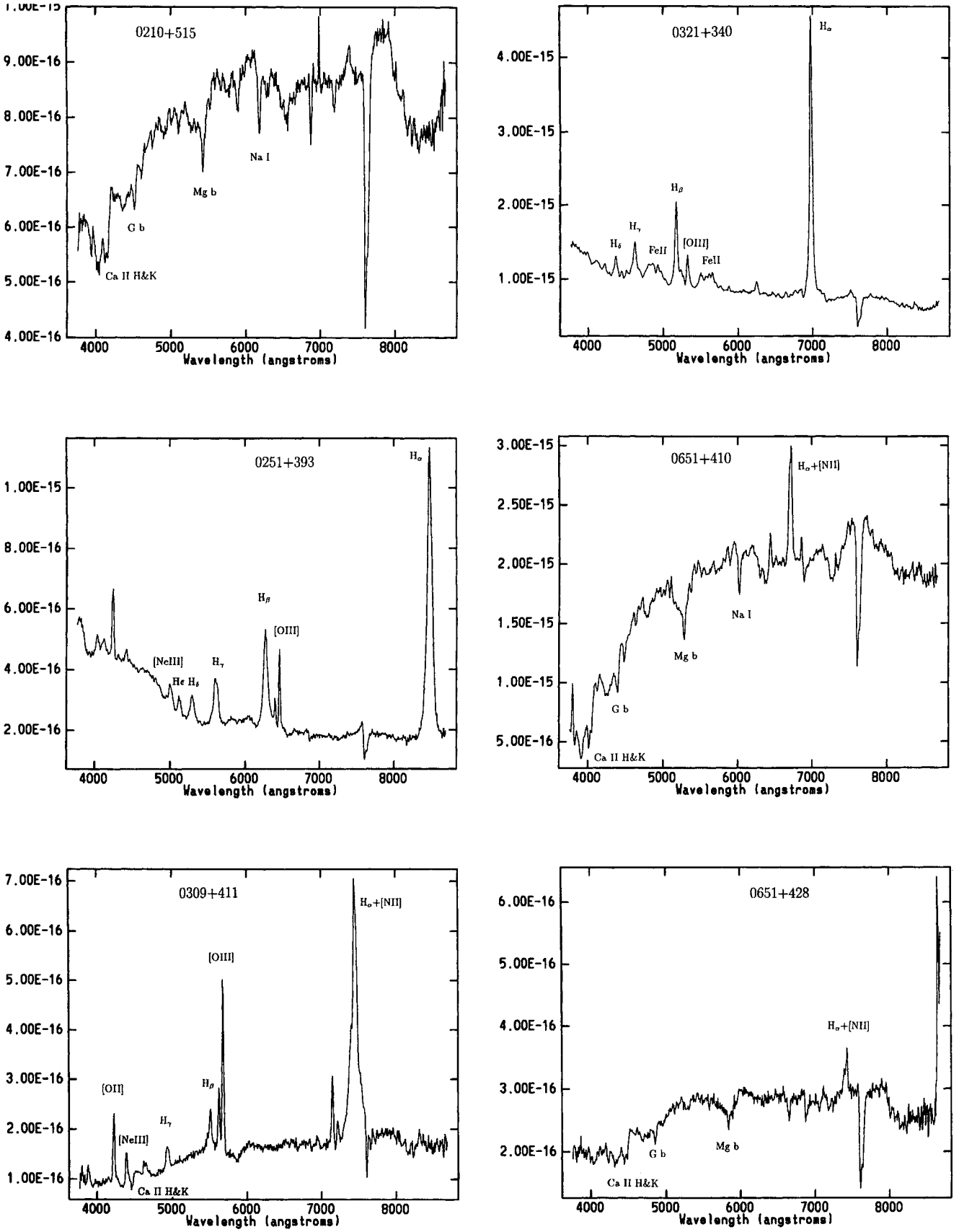

Figure 1 – *continued*

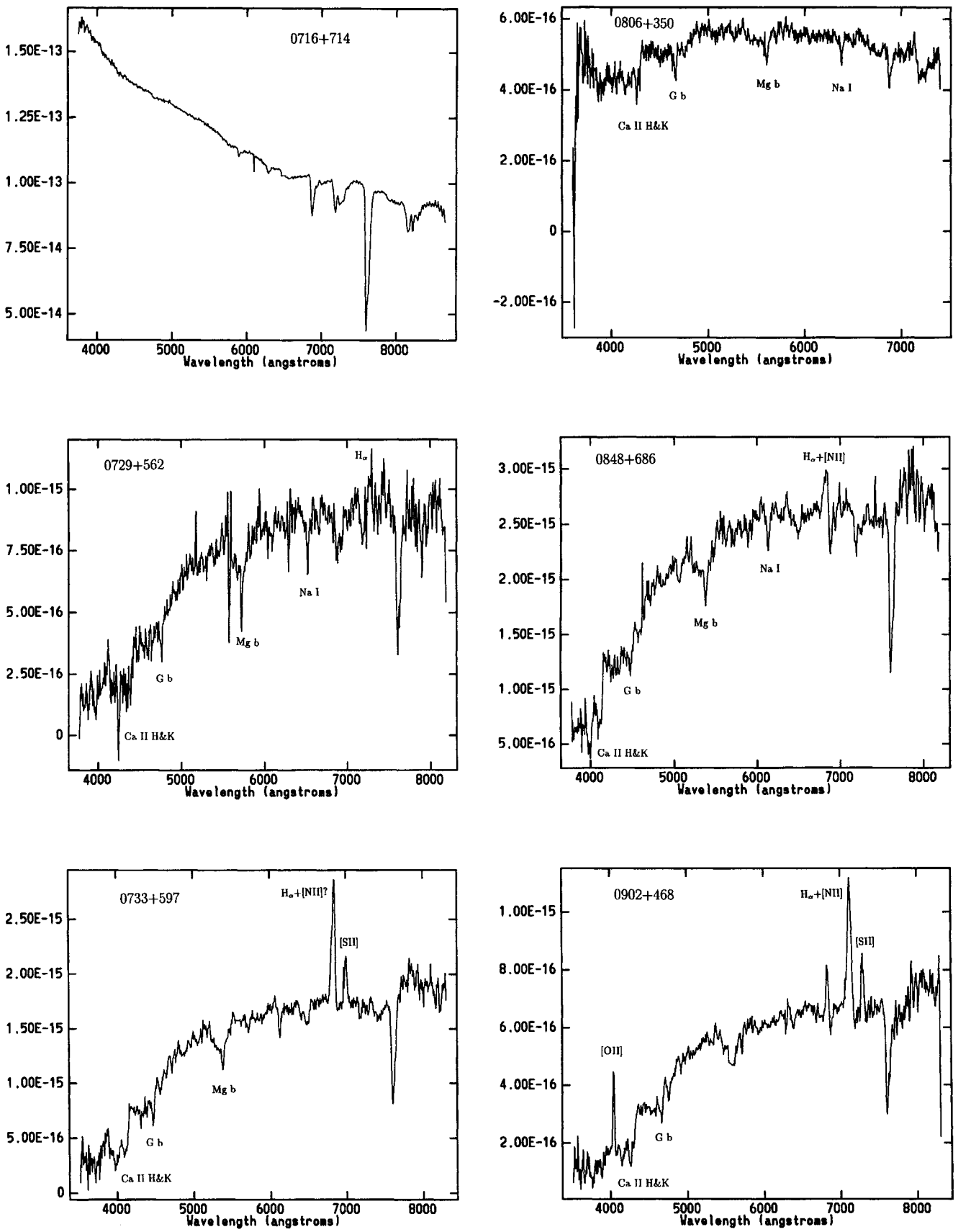

Figure 1 – *continued*

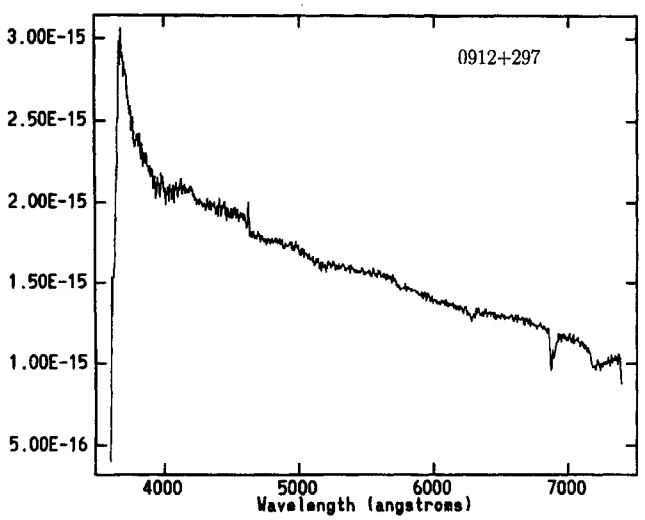

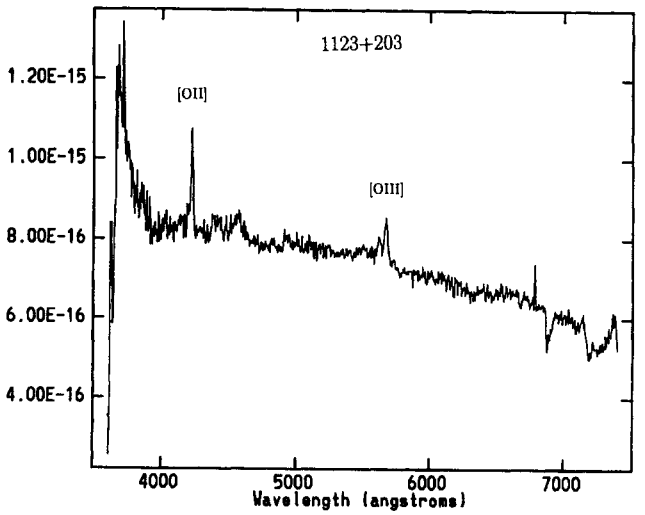

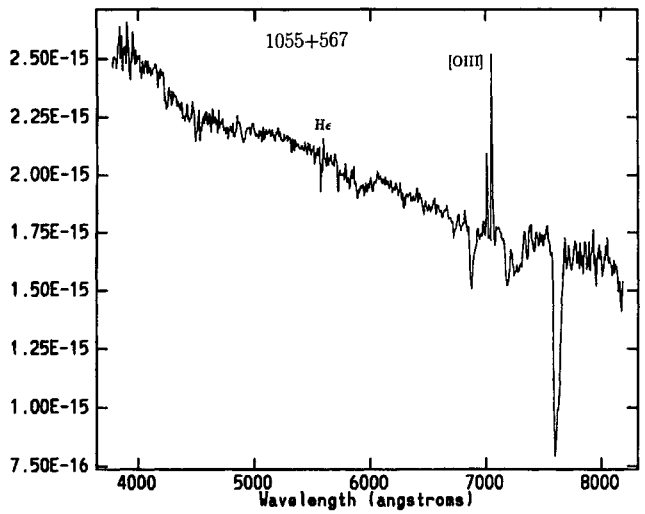

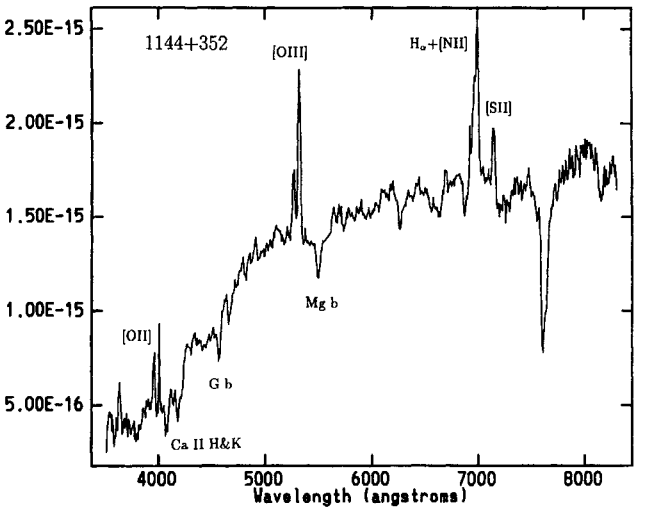

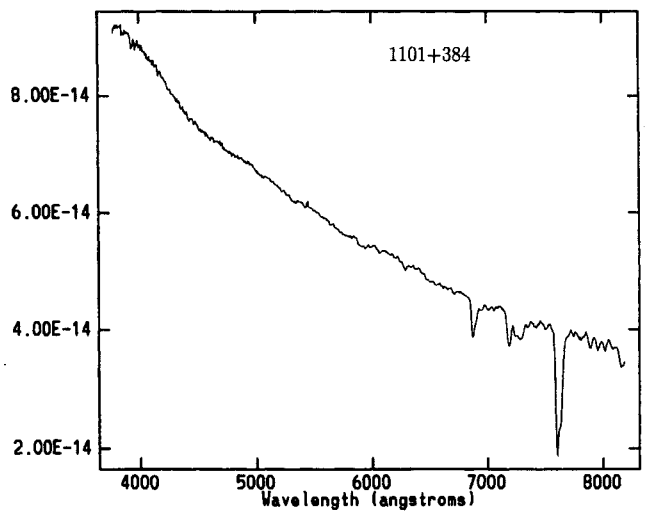

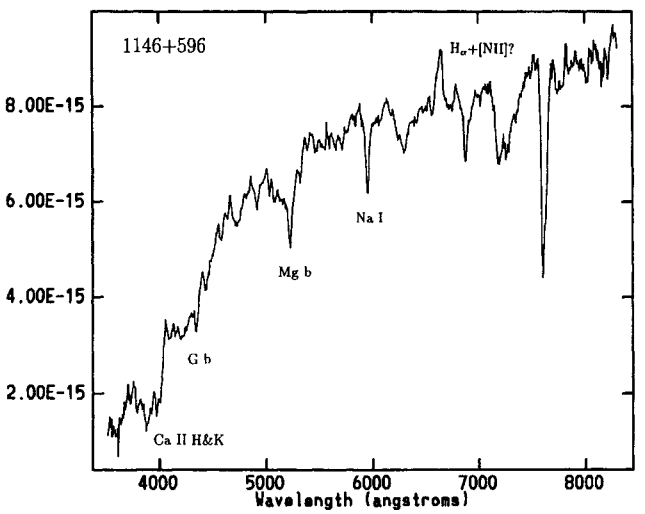

Figure 1 – *continued*

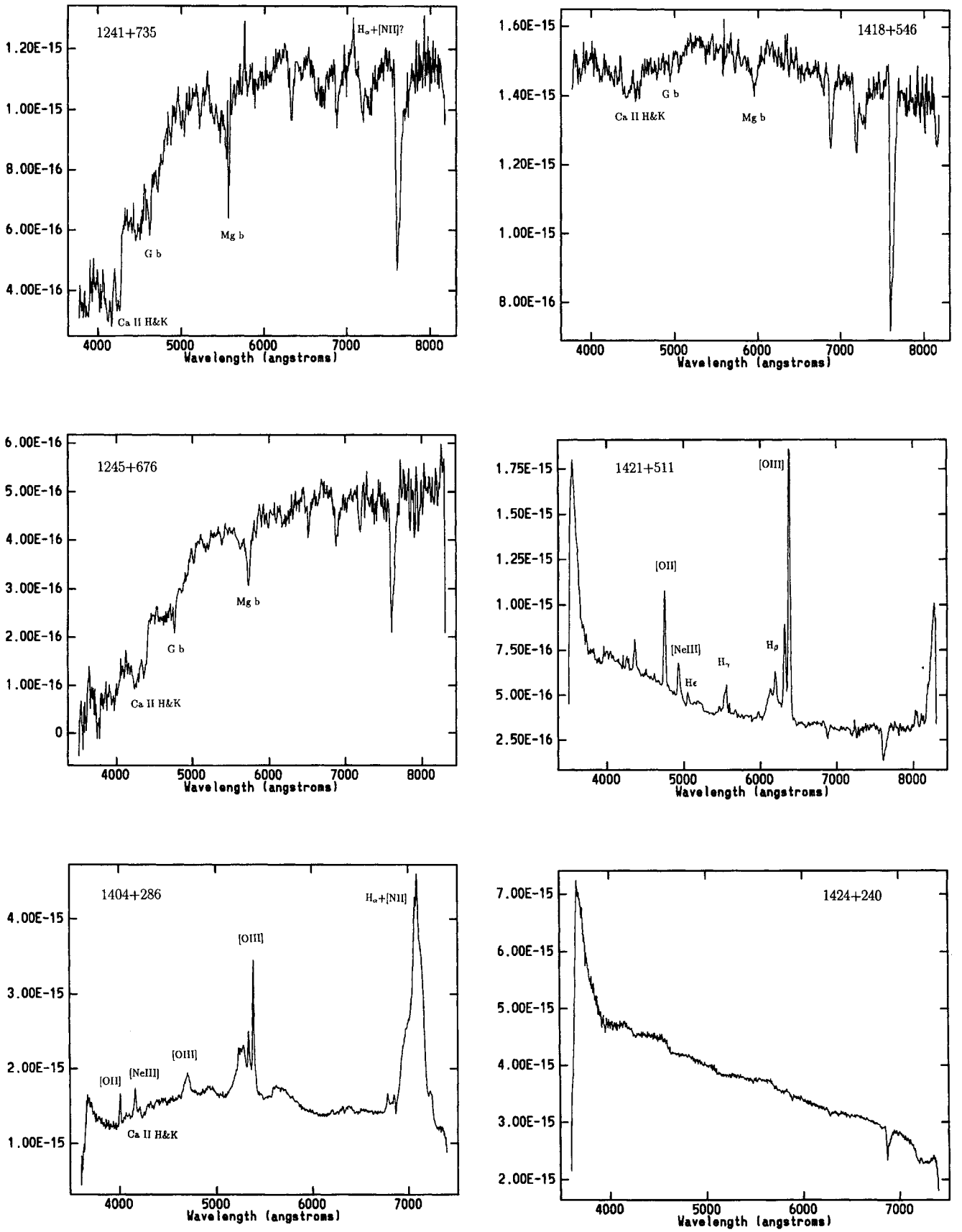

Figure 1 – *continued*

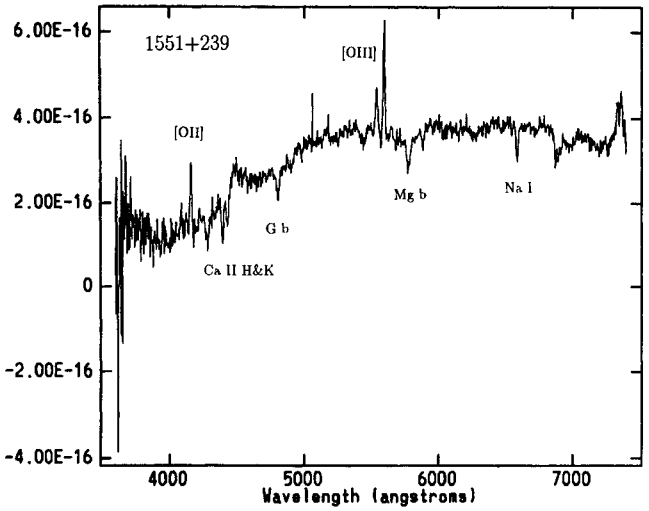

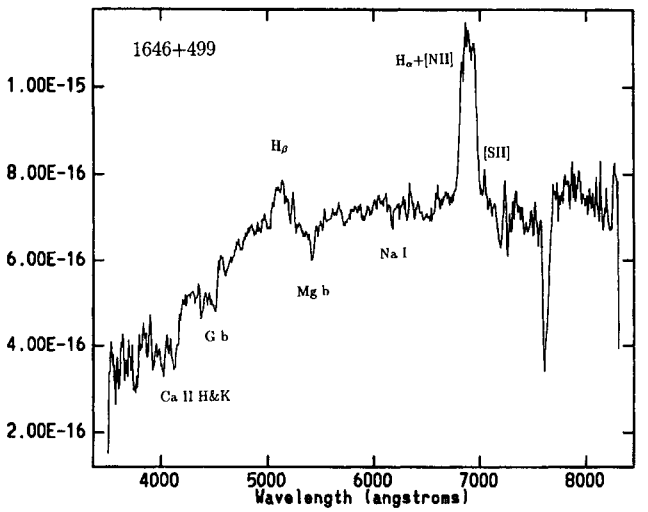

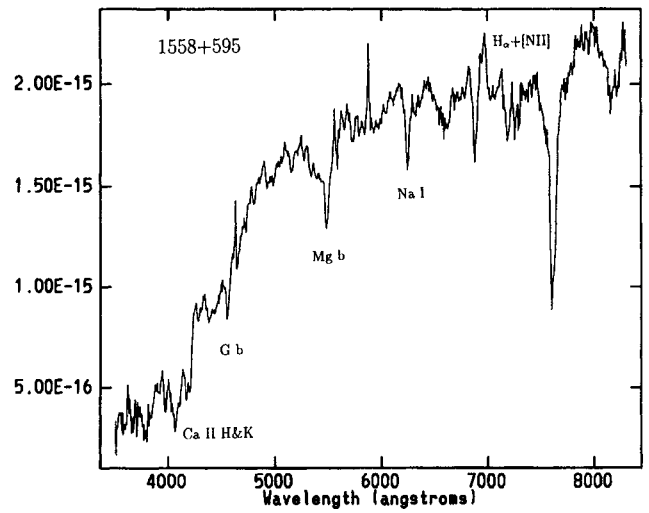

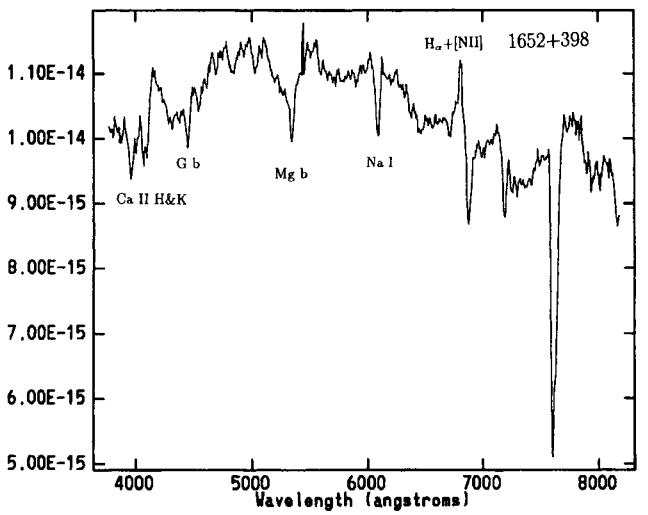

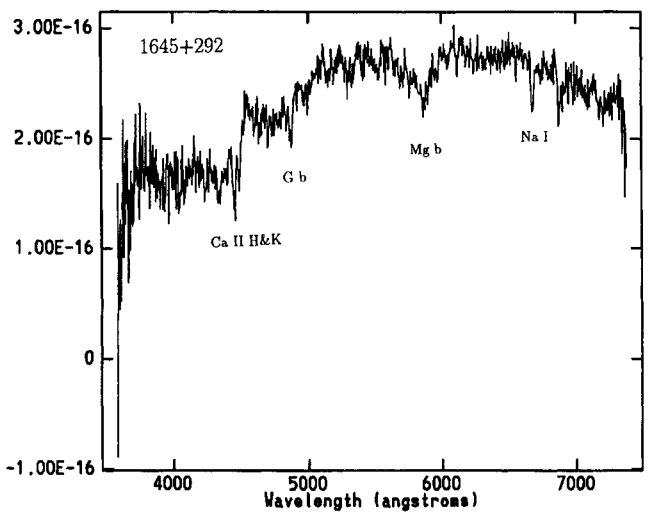

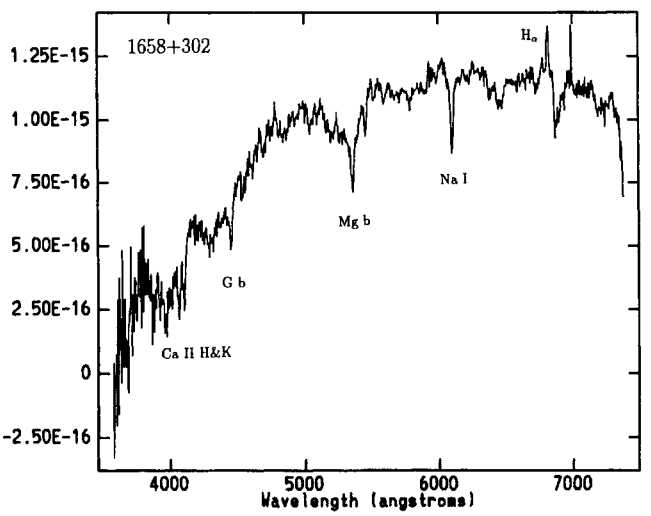

Figure 1 – *continued*

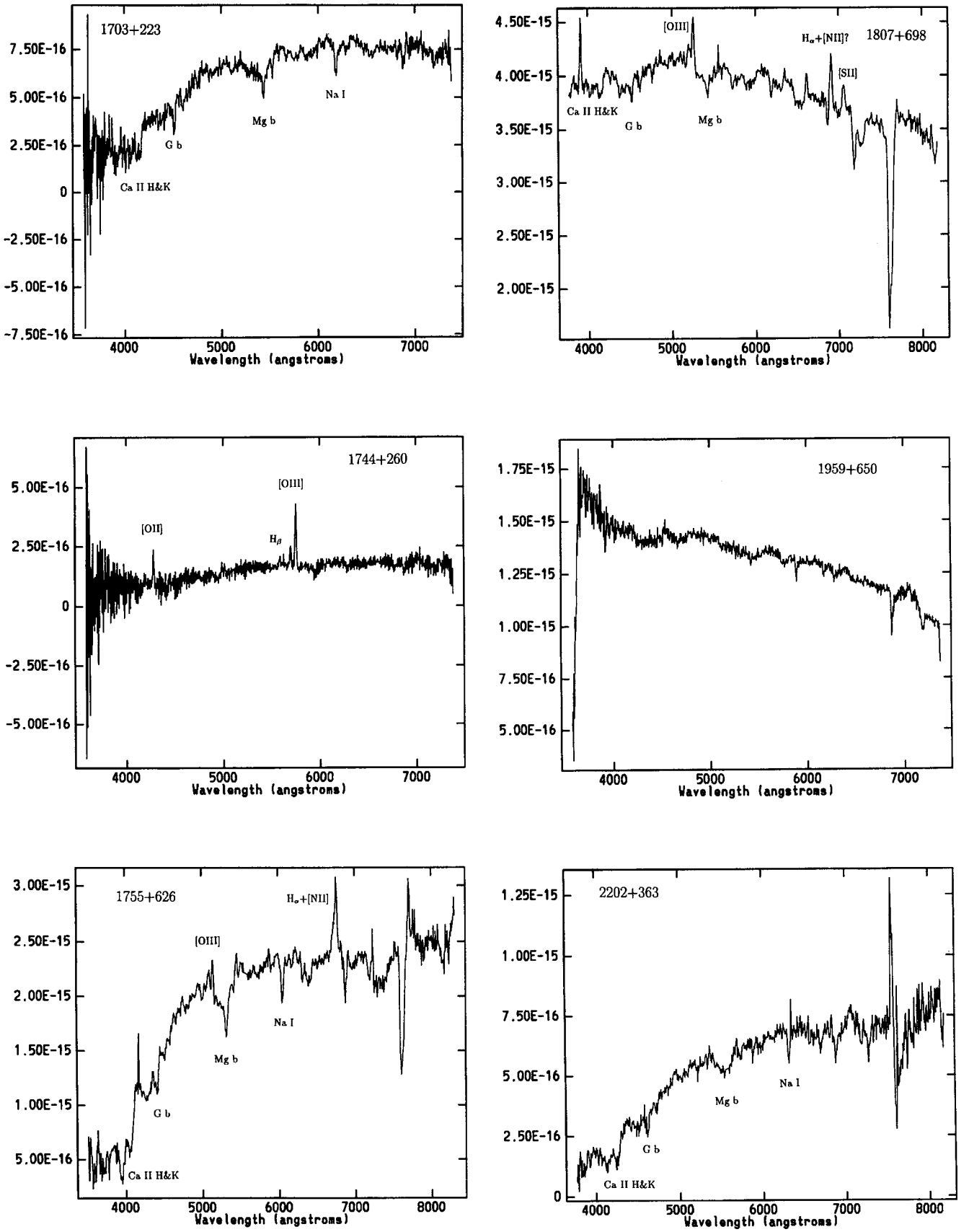

Figure 1 – *continued*

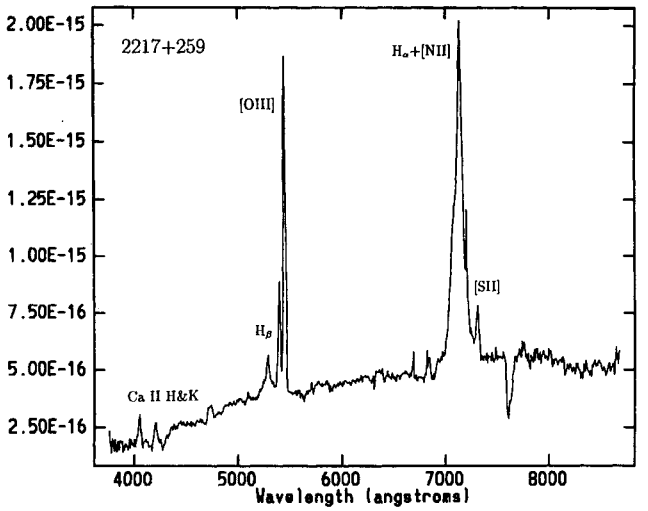

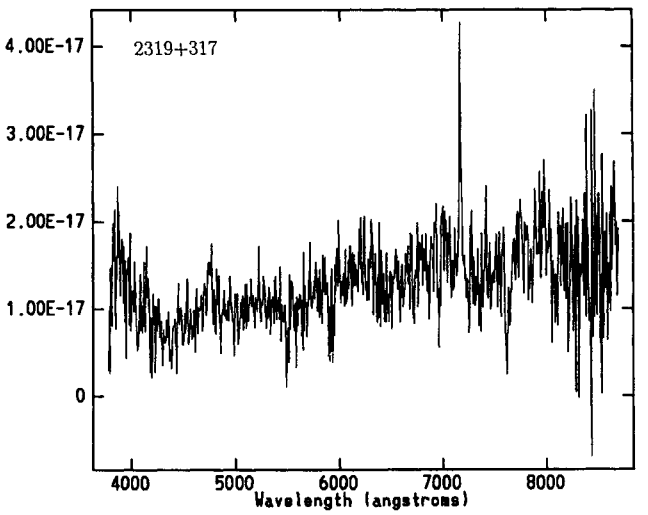

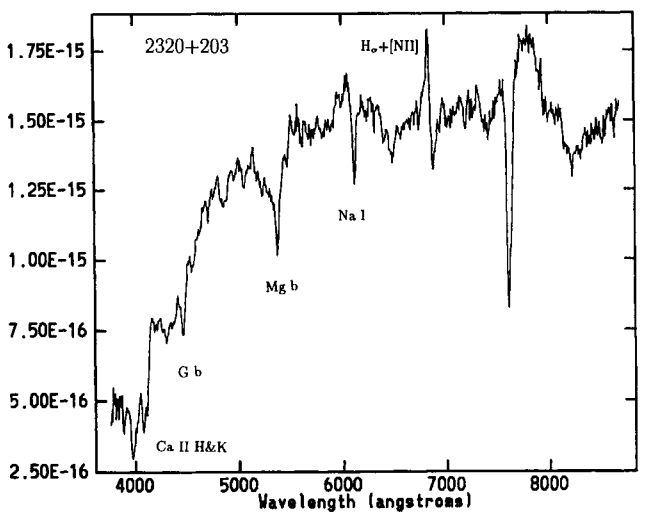

Figure 1 – *continued*

Most of these observations were made with the 'Two-Holer' polarimeter/photometer (Sitko, Schmidt & Stein 1985) and were unfiltered (these 'white light' observations are denoted by 'W' in the filter column of Table 2).

Two-Holer is a dual-beam polarimeter in which light entering an entrance aperture passes through a rapidly rotating, semi-achromatic $\lambda/2$ waveplate. The waveplate is rotated at 20.8 Hz and therefore modulates any incident linear polarization by 83.2 Hz. The beam is split by a Wollaston prism with each of the two orthogonally polarized beams then being detected by one of two RCA C31034 photomultiplier tubes (PMTs). Rapid modulation of the polarized light and the simultaneous sampling of both senses of polarization largely eliminates systematic effects, such as seeing variations and guiding errors, from affecting the polarimetry. In addition, the instrumental polarization has been measured to be <0.1 per cent at both telescopes. The PMTs have good quantum efficiencies (between 10 and 25 per cent in the optical spectral region) and, when cooled by dry ice, have low dark current (1–3 count s^{-1}). Linear polarization is detected by the PMTs as a sinusoidal modulation of the count rate, with the amplitude of the modulation proportional to the degree of polarization (P) and the phase related to the polarization position angle (θ). Observations of linear polarization standards (e.g. Schmidt, Elston & Lupie 1992) are used to transform the instrumental polarization position angle (PA) to a PA on the sky in the equatorial system.

In Table 2 we list the telescope and aperture used along with the data and time (UT), filter, normalized linear Stokes parameters (Q/I and U/I), 1σ uncertainty in the Stokes values, P, uncertainty in P, θ and the uncertainty in θ. Since P does not have a Gaussian error distribution (i.e., for low polarimetric S/N ratio, P tends to be overestimated), these values have been corrected for statistical bias using

$$P^2 = P_{\rm obs}^2 - P_{P,\rm obs}^2 .$$

If $P_{\rm obs}/\sigma_P < 1.5$, the polarization PA is not well determined and no value is given for θ. For $P_{\rm obs}/\sigma_P > 1.5$ we estimate σ_θ in the same manner as outlined by Sitko et al. (1985). Detailed descriptions of the data-taking and reduction procedures used with Two-Holer can be found in Smith et al. (1992) and Jannuzi, Smith & Elston (1993).

Starlight from the host galaxy of a radio source can greatly reduce the measured polarization of any optical counterpart to the radio nucleus if enough of this essentially unpolarized continuum is included in the observation aperture. Apertures employed for the optical polarimetry are listed by number (along with the telescope) in Tables 2 and 3. The aperture sizes are listed in Table 4. Note that '90-3' entered in Table 2 signifies observations made at the 90-inch telescope with the Steward Observatory 'Octopol' polarimeter (see Glenn et al. 1994). Both polarimeters are sensitive to light in the $\lambda\lambda$3200–8600 Å range and the effective wavelength for unfiltered observations is $\sim$5800 Å for an object with an optical spectral index of $\alpha \sim 1$ ($S_\nu \propto \nu^{-\alpha}$). A few filtered measurements were made and both polarimeters have filter sets consisting of Johnson *UBV* and Kron–Cousins *RI* glass filters. Also in Table 3 is the polarimetry of stars in the fields of several objects in the 200-mJy sample. These stars were observed to determine if interstellar polarization is important in these lines of sight through the

Table 2. Summary of the polarization measurements of the 200-mJy sample: (i) name of the object in B1950 coordinates; (ii) the telescope used and the corresponding aperture code (see Table 4); (iii) the Universal Time (UT); (iv) the filter used; (v) and (vi) the ratio of Stokes parameters Q/I and U/I, respectively; (vii) the standard deviation in Q/I (assumed $\sigma_{U/I}$); (viii) and (ix), respectively, the percentage polarization and its standard deviation. The percentage polarization preceded by $<$ represents 2σ upper limits.

Object (B1950)	tel.-apt.	UT Time yymmdd hh.mm	fil.	Q/I	U/I	σ(Q/I)	P (%)	σ(P)	θ (°)	σ(θ)
0035+227	90-0	920925. 8.52	W	-0.214	0.932	0.464	0.84	0.46	51.5	16.9
0046+316	90-0	920925. 9.09	W	-2.172	1.095	0.220	2.42	0.22	76.6	2.6
0046+316	90-0	920925. 9.38	B	-3.852	2.400	0.574	4.50	0.57	74.0	3.6
0046+316	90-0	920925. 9.59	I	-1.642	0.585	0.451	1.68	0.45	80.2	7.4
0116+319	90-0	920926.11.42	W	-0.113	0.339	0.395	<1.15			
0125+487	90-0	920925.10.26	W	-2.516	0.341	0.569	2.47	0.57	86.1	6.4
0149+710	90-0	920925.10.58	W	-2.512	2.191	0.366	3.31	0.37	110.6	3.1
0210+515	90-0	920925.11.24	W	-2.208	0.346	0.287	2.22	0.29	94.4	3.7
0251+393	90-0	920926. 7.07	W	-0.545	0.715	0.499	0.75	0.50	116.4	20.3
0309+411	90-0	920926. 7.47	W	1.062	0.334	0.502	0.99	0.50	171.3	15.3
0321+340	90-0	920926. 8.52	W	0.671	0.250	0.218	0.68	0.22	10.2	8.7
0651+428	90-0	920406. 3.16	W	0.920	1.292	0.348	1.55	0.35	27.3	6.3
0651+428	90-0	920408. 4.09	B	1.196	3.669	1.841	3.39	1.84	36.0	16.5
0651+410	90-0	920406. 4.02	W	0.458	0.165	0.133	0.47	0.13	9.9	7.8
0729+562	90-0	920406. 5.18	W	0.025	0.344	0.382	<1.11			
0733+597	90-0	920406. 5.50	W	0.065	0.229	0.231	<0.70			
0806+350	61-0	930417. 3.20	W	1.973	0.882	0.335	2.13	0.33	168.0	4.4
0848+686	90-0	920406. 6.15	W	0.669	0.360	0.176	0.74	0.18	14.1	6.6
0848+686	90-0	920408. 6.09	B	1.211	0.842	1.001	<3.48			
0902+468	90-0	920406. 6.43	W	0.339	0.293	0.374	<1.20			
0912+297	61-0	930326. 5.06	W	3.779	0.707	0.414	3.82	0.41	174.7	3.1
1055+567	90-0	920406. 7.04	W	2.550	0.134	0.218	2.54	0.22	178.5	2.4
1055+567	90-1	920407. 5.12	W	1.936	0.468	0.147	1.99	0.15	173.2	2.1
1055+567	90-0	920408. 5.39	W	1.875	0.059	0.203	1.86	0.20	0.9	3.1
1055+567	90-1	920407. 5.39	B	2.507	0.836	0.374	2.62	0.37	170.8	4.1
1055+567	90-1	920407. 7.27	V	2.218	0.200	0.277	2.21	0.28	177.4	3.6
1055+567	90-1	920407. 7.07	R	1.867	0.395	0.320	1.88	0.32	174.0	4.8
1055+567	90-1	920407. 6.33	I	2.060	0.196	0.331	2.04	0.33	177.3	4.6
1123+203	61-0	930417. 6.27	W	-1.654	1.815	0.278	2.44	0.28	66.2	3.2
1144+352	90-0	920406. 7.35	W	-0.038	0.228	0.197	<0.63			
1146+596	90-0	920406. 8.00	W	0.241	0.278	0.091	0.36	0.09	24.5	7.0
1146+596	90-0	920407. 8.24	B	0.362	0.577	0.426	0.53	0.43	29.0	24.0
1241+735	90-0	920406. 8.39	W	0.193	0.054	0.273	<0.75			
1245+676	90-0	920406. 9.16	W	0.447	-0.278	0.393	<1.31			
1404+286	61-0	930418. 8.34	W	0.331	0.231	0.259	0.31	0.26	17.4	24.9
1421+511	90-0	920406.10.00	W	-0.400	-0.347	0.364	<1.26			
1424+240	61-0	930326. 7.48	W	-0.681	4.021	0.218	4.07	0.22	130.2	1.5
1551+239	61-0	930326. 9.14	W	0.189	0.470	0.768	<2.04			
1558+595	90-0	920406.10.32	W	-0.268	0.052	0.256	<0.78			
1558+595	90-0	920407. 9.10	B	1.819	0.231	0.974	1.55	0.97	3.6	19.1
1558+595	90-0	920408. 8.24	B	0.862	2.293	1.126	2.18	1.13	34.7	15.7
1645+292	61-0	930326.10.44	W	0.987	-1.589	0.472	1.81	0.47	119.1	7.2
1646+499	90-0	920406.11.00	W	1.453	1.635	0.247	2.17	0.25	65.8	3.2
1646+499	90-0	920407. 9.55	W	0.195	-0.041	0.239	<0.68			
1646+499	90-0	920408. 9.56	W	-0.104	1.004	0.184	0.99	0.18	48.0	5.2
1646+499	90-1	920408.11.19	B	-1.244	1.231	0.414	1.70	0.41	67.7	6.8
1658+302	90-3	930425.10.50	W	-0.065	-0.310	0.241	<0.80			
1703+223	61-0	930418. 9.58	W	-0.484	-0.151	0.269	0.43	0.27	98.7	19.1
1744+260	90-3	930425.11.20	W	-0.803	0.526	0.983	<2.93			
1755+626	90-0	920406.11.52	W	-0.503	-0.124	0.319	0.41	0.32	96.9	23.5
1755+626	90-0	920407.11.04	B	0.030	0.022	0.787	<1.61			
1959+650	90-0	920925. 3.45	W	2.463	-1.613	0.414	2.92	0.41	163.4	4.0
2116+81	90-3	930425.11.07	W	0.782	-0.568	0.211	0.94	0.21	162.0	6.3
2214+201	90-3	930426.11.19	W	-0.640	0.333	0.418	0.59	0.42	76.3	21.6
2202+363	90-0	920925. 4.59	W	-0.623	-0.046	0.338	0.52	0.34	92.1	19.6
2217+295	90-0	920925. 7.13	W	-0.065	5.020	0.476	5.00	0.48	45.4	2.7
2217+259	90-0	920925. 7.24	B	2.726	2.533	2.947	<9.62			
2217+259	90-0	920925. 7.40	I	0.667	4.342	0.622	4.35	0.62	40.6	4.1
2319+317	90-0	920925. 8.06	W	-0.077	1.847	7.179	<16.21			

galaxy. The stars were picked at random and therefore their polarization must be viewed as a lower limit to the interstellar polarization in the direction of the AGN. In Fig. 2 we plot the distribution of the reference star polarization.

4 RESULTS

Information of the sources is collected in Table 5 which lists: (i) the name of the object (B1950); (ii) the redshift which is the straight average value obtained from the identified

Table 3. Summary of the polarization measurements of the reference stars in the fields of the sources of the 200-mJy sample. The columns are the same as in Table 2.

Object (B1950)	tel.-apt.	UT Time yymmdd hh.mm	fil.	Q/I	U/I	σ(Q/I)	P (%)	σ(P)	θ (°)	σ(θ)
STAR A(0046)	90-1	920925. 9.18	W	-0.713	0.563	0.138	0.90	0.14	109.2	4.3
STAR B(0046)	90-1	920925. 9.25	W	-0.676	0.652	0.145	0.93	0.15	112.0	4.4
STAR A(0125)	90-1	920925.10.37	W	-0.898	0.069	0.126	0.89	0.13	87.8	4.0
STAR B (0125)	90-1	920925.10.44	W	-1.371	0.106	0.235	1.35	0.23	92.2	4.9
STAR A(0149)	90-1	920925.11.05	W	-0.717	-0.309	0.153	0.77	0.15	101.7	5.6
STAR B(0149)	90-1	920925.11.11	W	-0.813	-0.698	0.196	1.05	0.20	110.3	5.2
STAR A(0210)	90-1	920925.11.31	W	-1.083	-0.481	0.058	1.18	0.06	102.0	1.4
STAR A(0251)	90-1	920926. 7.18	W	-0.566	-0.471	0.312	0.67	0.31	109.9	14.0
ST A(0651+42)	90-0	920406. 3.35	W	0.486	0.340	0.171	0.57	0.17	17.5	8.2
ST B(0651+42)	90-1	920406. 3.43	W	0.468	0.137	0.161	0.46	0.16	8.2	9.5
STAR A(0806)	61-0	930417. 3.52	W	0.310	0.218	0.246	0.29	0.25	17.6	25.3
STAR B(0806)	61-1	930417. 4.12	W	0.187	-0.145	0.096	0.22	0.10	161.1	13.2
ST A(0848+68)	90-1	920406. 6.30	W	0.258	0.141	0.046	0.29	0.05	14.4	4.5
STAR A(0912)	61-1	930326. 5.19	W	-0.020	0.081	0.105	<0.29			
STAR B (0912)	61-0	930326. 5.29	W	-0.498	0.614	0.368	0.70	0.37	64.5	16.0
ST A(1055+56)	90-1	920406. 7.13	W	0.059	0.004	0.047	<0.15			
ST B(1055+56)	90-1	920406. 7.19	W	0.022	0.232	0.162	<0.56			
ST C(1055+56)	90-1	920407. 7.47	W	-0.212	0.106	0.201	<0.64			
STAR A(1123)	61-1	930417. 6.51	W	0.002	-0.045	0.139	<0.32			
STAR B(1123)	61-1	930417. 7.00	W	-0.012	-0.219	0.091	0.20	0.09	133.4	13.6
ST A(1146+59)	90-1	920406. 8.18	W	-0.042	-0.010	0.088	<0.22			
STAR A(1424)	61-1	930326. 8.02	W	-0.152	-0.091	0.215	<0.61			
STAR B(1424)	61-1	930326. 8.10	W	0.072	-0.038	0.259	<0.60			
ST A(1558+59)	90-1	920408. 9.08	W	0.009	-0.050	0.126	<0.30			
STAR A(1645)	61-1	930326.11.59	W	-0.749	-0.304	0.334	0.74	0.33	101.1	13.6
STAR B(1645)	61-1	930326.12.09	W	-1.571	-0.733	0.487	1.66	0.49	102.5	8.1
ST A(1646+49)	90-1	920406.11.22	W	0.127	0.222	0.209	<0.67			
ST B(1646+49)	90-1	920406.11.33	W	0.162	0.086	0.098	0.15	0.10	14.0	19.3
STAR A (1959)	90-0	920925. 3.51	W	-0.414	-0.645	0.434	0.63	0.43	118.6	20.9
STAR A (2202)	90-1	920925. 5.14	W	-0.083	0.507	0.094	0.51	0.09	49.7	5.2

Table 4. Aperture sizes on the telescopes of the Steward Observatory (SO). The codes of the aperture sizes in mm (column 2), and arcsec (columns 3 and 4) are given for the two SO telescopes used for the polarimetry in the course of this work.

apt. code	apt.size (mm)	apt. size (") on 1.54 m	apt. size (") on 2.3 m
0	0.51	5.1	2.9
1	0.94	9.4	5.3
3	0.29	–	2.9

features seen in our spectra and, in the case where no observations were made, the redshift obtained from published sources is quoted in parentheses; (iii) the standard deviation in the redshift measurement; (iv) optical polarization percentages (in the case where $<$ appears it means that only a 2σ upper limit was established for the measurement; refer to the polarizations given in Table 2); (v) the estimate of the 4000-Å break contrast defined as

$$\frac{f^+ - f^-}{f^+}, \tag{1}$$

where f^+ and f^- are respectively the flux redward and blueward of the break; (vi) the estimate of the EW for the strongest emission line in the spectrum (in the case of the seven featureless BL Lacs an upper limit of 2 Å was estimated); (vii) the percentage polarization at 8.4 GHz of the compact radio core (from Akujor & Patnaik 1993; A. Patnaik, private communication); (viii) the 'eye' magnitude estimates on the red POSS plate (we intend to get magnitude measurements for this sample); (ix) whether the object is a known BL Lac (BL), or a source with a Seyfert-type spectrum (BLRG for broad lines and NLRG for narrow lines); and finally in (x) the reference to a note on the source. All the quantities shown in parentheses are the ones taken from the literature.

5 DISCUSSION

Our goal is to investigate possible limits on the BL Lac phenomenon. With this in mind, we investigate the distribution of observed properties of the 200-mJy sample and look for any breaks that may occur. We discuss the distribution of objects according to four parameters: the percentage optical polarization, the percentage radio core polarization, the 4000-Å break contrast and the EW of emission lines.

The question we are trying to address is whether or not the observations indicate the presence of extra continuum emission other than from stars, and, if they do, is this non-thermal (BL Lac) emission or the type normally associated with a Seyfert-type nucleus? The most direct way of testing for the presence of this extra continuum is through the measurement of the 4000-Å break contrast, or through the detection of optical polarization. In the case of the break contrast the working assumption is that all the hosts of these radio-loud objects are early-type galaxies. For these, it is observationally well established that the 4000-Å break contrast spans a small range in values. For example, Dressler & Schectman (1987) have studied more than 700 early-type

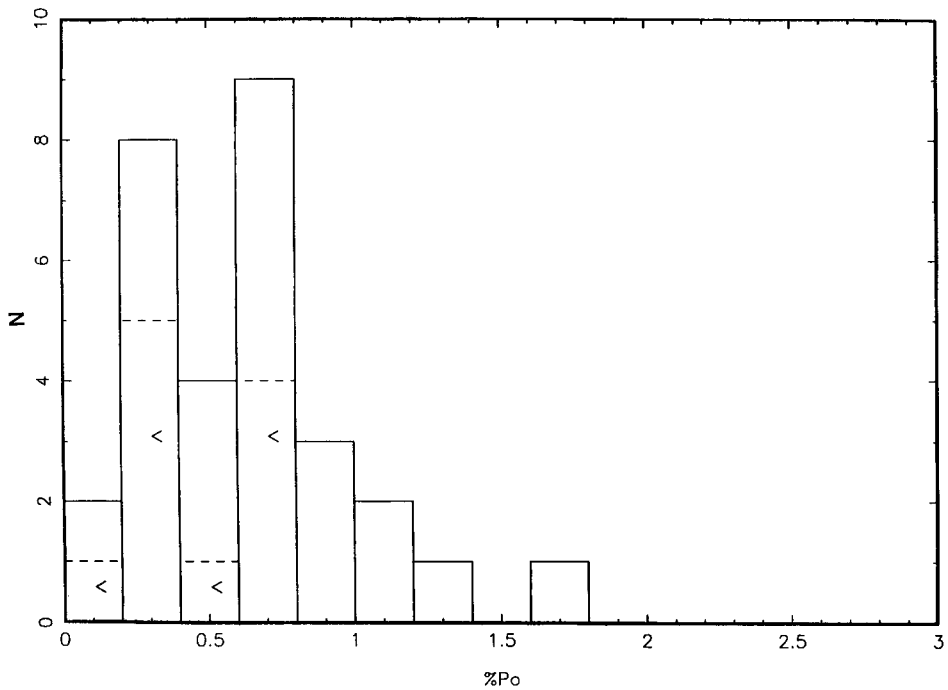

Figure 2. Distribution of percentage optical polarization for the reference stars in the field of objects of the 200-mJy sample. Dashed bins with the < symbol correspond to upper limit values.

galaxies, and they find a mean break contrast of 0.49. From examination of their data we find that less than 5 per cent of these galaxies have break contrast ≤ 0.4. It is therefore a reasonable presumption that a galaxy with a measured break contrast less than 0.4 has some extra source of continuum. (In principle, there is no reason why those objects with break contrast > 0.4 should not hold extra sources of continuum. However, these will not be detected via the measure of contrast, or any other quantity that is contrast-dependent.)

High percentage polarization (≥ 2 per cent) is also a clear diagnostic of emission other than that from stars. This level of polarization can be because of either non-thermal BL Lac continuum, or (scattered) emission from a Seyfert-type nucleus. We distinguish those objects with a Seyfert-type continuum from those with a BL Lac continuum by using the EW of emission lines, since, empirically, the former is always associated with the presence of strong emission lines.

The last parameter we will discuss is the radio core polarization. Gabuzda & Cawthorne (1993) suggest that the percentages of radio core polarizations for radio galaxies, quasars and BL Lacs are systematically different, with values increasing from radio galaxies, through quasars, to BL Lac objects. This may be a useful parameter to help the distinction between the BL Lacs and the other types of objects in the 200-mJy sample (especially among those objects with contrast > 0.4), and it will be discussed in Section 5.4. In the following sections we examine how the analysis of these four parameters can be used to help establish a BL Lac sample.

5.1 Break contrast and optical polarization

Fig. 3 shows the distributions of break contrast for 50 objects (a), and the percentage optical polarization for 49 objects (b). The contrast distribution is clearly bimodal with clusters of objects in the ranges 0–0.1 and 0.4–0.5. Since it is known from the work of Dressler & Shectman (1987) that less than 5 per cent of early-type galaxies have break contrast ≤ 0.4 (see the previous section), it seems natural to regard those objects in the sample that have values of break contrast below that value as having an extra component to the continuum emission. It is not, however, possible to tell if this extra continuum is from a BL Lac, or a Seyfert-type nucleus. To discriminate between the two possibilities it is necessary to use other diagnostics as will be discussed later in Section 5.3.

The polarization distribution (Fig. 3b), on the other hand, does not show any bimodality. Instead, the majority of objects form a large peak at low values and a long tail of high-polarization objects. Interstellar polarization can be as high as 2 per cent (see Fig. 2). It is therefore, only possible to identify with confidence objects with $P_o \geq 2$ per cent as being intrinsically polarized.

The two parameters, break contrast and percentage of optical polarization, are expected to be correlated in a two-component model for the continuum. In fact, if a continuum component of intrinsic percentage polarization P_{int} is diluted by different amounts of unpolarized starlight, then the observed value P_{obs} is given by

$$P_{obs} = (1 - 2C) P_{int}, \qquad (2)$$

Table 5. Properties of the 200-mJy sample: (i) the name of the object (B1950); (ii) the average redshift (the redshift from the reference is shown in parentheses when one was not measured); (iii) the standard deviation in the redshift measurement; (iv) optical polarization percentages (in the case where < appears it means that only a 2σ upper limit was established for the measurement; refer to the polarization Table 2 for details); (v) the estimate of the 4000-Å break contrast; (vi) the estimate of the EW for the strongest emission line in the spectrum (observer's frame); (vii) the percentage of peak radio polarization at 8.4 GHz; (viii) the 'eye' magnitude estimates on the red POSS plate (we intend to get magnitude measurements for this sample); (ix) whether the object is a known BL Lac (BL), or a source with a Seyfert-type spectrum (BLRG for broad lines and NLRG for narrow lines); and finally (x) notes on individual sources. The ? symbols correspond to the cases where no information is available.

Name (B1950)	z	σ_z	P_o (%)	contrast	EW (Å)	P_r (%)	m_r	class.	Notes
0035+227	0.096	0.002	0.84	0.46	EW(Hα)=8.1	< 0.07	16.5		
0046+316	0.015	0.001	2.42	≤ 0.3	EW([OIII]$_2$)=454	0.73	15.0	NLRG	
0055+300	0.015	0.002	?	0.46	EW(Hα+[NII])=13.5	0.13	12.5		
0109+224	—	–	(10.2)[a]	–	≤ 2	2.73	15.5	BL	
0116+319	0.060	0.001	<1.15	0.45	EW(Hα+[NII])=18	0.2	16.0		
0125+487	0.067	0.001	2.47	0.22	EW(Hα+[NII])=58	1.9	17.0		1
0149+710(*)	0.022	0.001	3.31	0.33	EW(Hα+[NII])=17.4	0.93	15.5		2
0210+515(*)	0.049	0.002	2.22	0.15	EW < 3	2.87	16.5		3
0251+393	0.289	0.001	0.75	≤ 0.15	EW(Hα)=959	0.87	17.0	BLRG	
0309+411	0.134	0.002	0.99	∼0.2	EW(Hα+[NII])=506	0.13	17.0	BLRG	
0316+41	(0.017)[b]	–	(0.6)[c]	0.1[o]	(EW([OIII]$_2$)=410)[o]	0.0	12.5	BLRG	4
0321+340	0.061	0.001	0.68	≤0.1	EW(Hα)=491	3.47	15.5	NLRG	
0651+410	0.021	0.002	0.47	0.39	EW(Hα+[NII])=30	< 0.2	15.0		5
0651+428	0.126	0.002	1.55	0.17	EW(Hα+[NII])=8	0.53	17.0		5
0716+714	–	–	(12.5)[a]	–	≤ 2	2.47	15.0	BL	
0729+562	0.104	0.001	<1.11	0.45	EW(Hα)=9	< 0.53	17.0		
0733+597	0.041	0.0015	<0.70	0.49	EW(Hα+[NII])=44	< 0.27	15.0		
0806+350	0.082	0.001	2.13	0.18	< 5	1.4	17.0		5
0848+686	0.039	0.001	0.74	0.47	EW(Hα+[NII])=6.5	< 1.2	14.5		
0902+468	0.084	0.003	<1.20	0.48	EW(Hα+[NII])=47	< 0.33	17.0		
0912+297	–	–	3.82	–	≤ 2	1.13	16.5	BL	
1055+567	0.410	–	2.54	≤0.05	EW([OIII]$_2$)=7	0.8	16.0		5
1101+384	(0.031)[b]	–	(3.7)[e]	(0.24)[f]	< 5	0.67	13.0	BL	
1123+203	0.133	0.001	2.44	≤0.05	EW([OII])=8	0.8	17.0		5
1133+704	(0.046)[b]	–	(3%)[n]	(0.31)[f]	< 5	2.4	14.5	BL	
1144+352	0.063	0.002	<0.63	0.37	EW(Hα+[NII])=25	2.8	15.5		5
1146+596	0.009	0.001	0.36	0.47	EW(Hα+[NII]?)=10	< 0.13	12.0		
1147+245	–	–	(6.2)[a]	–	≤ 2	1.6	17.0	BL	
1215+303	–	–	(8.0)[a]	–	≤ 2	2.6	15.0	BL	
1217+295	(0.002)[b]	–	?	(0.42)[g]	(EW(Hα=22.3)[h]	< 0.13	11.0		
1219+285	(0.102)[b]	–	(4.3)[a]	?	(EW(Hα)∼ 1)[i]	0.53	15.0	BL	
1241+735	0.075	0.001	<0.75	0.43	EW(Hα+[NII]?)=7.4	< 0.53	15.0		
1245+676	0.103	0.006	<1.31	0.48	< 5	< 0.53	17.0		
1254+571	(0.041)[b]	–	?	(0.0)[j]	(EW(Hα=700)[j]	< 0.27	14.0	BLRG	
1404+286	0.075	0.0015	<0.31	0.09	EW(Hα+[NII])=460	0.47	15.0	BLRG	
1418+546	0.151	0.004	(7.5)[a]	0.03	EW([OIII]$_2$)=0.8	1.53	15.5	BL	
1421+511	0.274	0.002	<1.26	≤0.1	EW([OIII]$_2$)=292	< 0.33	17.0	BLRG	
1424+240	–	–	4.07	–	≤ 2	1.6	16.0	BL	
1532+236	(0.018)[b]	–	?	?	(EW(Hα ∼ 60)[k]	< 0.6	14.0		
1551+239	0.115	0.002	<2.04	0.27	EW([OIII]$_2$)=15	0.47	16.5		5
1558+595	0.057	0.001	<0.78	0.43	EW(Hα+[NII])9.4	< 0.53	15.0		
1645+292	0.132	0.001	1.81	0.19	< 5	2.13	17.0		5
1646+499	0.045	0.002	Pvar	0.22	EW(Hα+[NII])=52	1.07	17.0		6
1652+398	0.031	0.003	(3.0)[c]	0.07	EW(Hα+[NII])=6.6	0.4	13.0	BL	
1658+302	0.036	0.0	<0.80	0.45	EW(Hα+[NII]?)=4.6	< 0.13	15.0		
1703+223	0.049	0.003	0.43	0.35	< 5	0.53	14.5		5
1744+260	0.147	0.0015	<2.93	≤0.3	EW([OIII]$_2$)=42	1.07	17.0		
1755+626	0.024	0.001	0.41	0.44	EW(Hα+[NII])=15	< 0.47	14.0		
1807+698	0.046	0.003	(8.0)[c]	0.025	EW(Hα+[NII?)=4	1.8	14.0	BL	
1959+650	–	–	2.92	–	≤ 2	0.6	16.5	BL	7
2116+81	0.084	0.001	0.94	≤0.25	(EW(Hα)=557)[l]	0.27	16.0	BLRG	
2202+363	0.073	0.003	0.52	0.41	< 5	< 0.2	16.5		
2214+201	?	?	0.59	?	?	8.3	17.0		8
2217+259	0.085	0.002	5.0	0.31	EW(Hα+[NII]?)=200	0.13	16.0	BLRG	
2319+317	?	?	<16.21	?	?	0.93	17.0		9
2320+203	0.038	0.002	?	0.47	EW(Hα+[NII]?)=14	0.73	14.5		
2337+268	(0.0322)[m]	?	?	?	?	0.4	14.5		

Note to Table 5:

(a) Wills et al. (1992); (b) Véron-Cetty & Véron (1991); (c) Impey, Lawrence & Tapia (1991); (d) Véron (1978); (e) Wills et al. (1980); (f) Ulrich (1978); (g) Heckman, Black & Crane (1980); (h) Filippenko (1985); (i) Weistrop et al. (1985); (j) Boksenberg et al. (1977); (k) Armus, Heckman & Miley (1989); (l) Stickel, Kühr & Fried (1993); (m) Sparks et al. (1986); (n) Angel & Stockman (1980); (o) F. Owen, private communication.

Notes on individual sources.

(1) *0125+487.* This source is interesting because its spectrum shows Hα emission which may be broad, probably blended with [N II], and also a weak enough 4000-Å break contrast of 0.22 to qualify the object as a BL Lac. The object shows polarized flux above 2 per cent, only part of which is likely to be intrinsic, since one of the nearby reference stars shows polarization above the 1 per cent level.

(2) *0149+710 (*).* This source is not part of the 200-mJy sample because it has $|b| < 12°$. However the 3.3 per cent optical polarization and break contrast of 0.33 suggest that this source is a BL Lac candidate.

(3) *0210+515 (*).* This is another source that does not belong to the 200-mJy sample because $|b| < 12°$. However, there are no strong emission lines in its spectrum and its observed break contrast is 0.15. Furthermore, the object showed polarization above the 2 per cent level, and above that of the reference star. This source satisfies all the criteria to be classified as a new BL Lac.

(4) *0316+41 (3C 84, NGC 1275).* This source is part of a complex system and it has been classified both as a Seyfert and as a BL Lac [see Shields & Oke (1975) and Véron (1978) for a discussion]. EWs for [O III] λ5007 Å have been reported to be ∼5 Å (Véron 1978), and the source is classified as a BL Lac with $z=0.017$ and magnitude $V=12.5$ in Véron-Cetty & Véron (1991). Recently, however, F. Owen (private communication) has obtained a spectrum that shows clearly the strong emission line of [O III] λ5007 Å with estimated EW of ∼510 Å. They also measured $D(4000)$ which is an index that measures the strength of the 4000-Å break and which corresponds to a break contrast of 0.1 as defined in this paper.

(5) *BL Lacs and BL Lac candidates.* All these sources except 0651+410 are BL Lacs and BL Lac candidates and are discussed in detail in the text (see Section 5.3).

(6) *1646+499.* This peculiar source is similar to 0125+487, with variable optical polarization on consecutive nights. Furthermore, its spectrum showed broad Hα emission and a low 4000-Å break contrast.

(7) *1959+650.* This source has been independently identified as an X-ray-selected BL Lac from the *Einstein* IPC Slew survey (Schachter et al. 1993). Its spectrum was observed to be featureless and its polarization larger than 2 per cent (well above that of the reference star).

(8) *2214+201.* The object was identified with a red stellar object of magnitude 17 on the POSS plate. observations of this source were not possible in the course of this project but previous radio measurements indicate that the spectrum of the object is marginally steeper than 0.5 (White & Becker 1992; Becker, White & Edwards 1991).

(9) *2319+317.* This object was identified with a red stellar object of magnitude 16.8 on the POSS plate. However, the source proved to be highly variable since the spectrum obtained corresponds to a magnitude much fainter than this (around 20 mag). Furthermore, no lines could be identified from this spectrum because of the low S/N ratio.

where C is the break contrast. Hence, if this simple picture is correct, we expect to find the high-contrast objects with lower percentage optical polarization and vice versa. In fact, when we plot contrast against percentage polarization for the 46 objects that have the relevant data in Fig. 4, it becomes clear that the majority of objects with polarizations above 2 per cent have small values of break contrast and vice versa. We note that the polarization observations were not simultaneous with the spectroscopic observations (a typical gap of 1 yr). Thus, variability can mean that a prominent continuum component at one epoch can fade from view at another. Nevertheless we plot in Fig. 4 the two trajectories of points expected from equation (2) for $P_{\rm int}$ of 2 per cent (dashed line) and 13 per cent (solid line). The data are entirely consistent with this range of intrinsic polarizations. We point out that if there are, as the data indicate, objects with an extra continuum component with intrinsic polarizations of ∼2 per cent, then measuring the break contrast may be a more sensitive way of identifying such components than measuring their percentage polarization. The reason for this is that, in an object for which the extra continuum is polarized at roughly 2 per cent, any starlight dilution will soon reduce this below the detection limit set by interstellar polarization. Therefore, it is possible that BL Lac objects with percentage optical polarizations below 2 per cent might be identified because of their low break contrast.

Another interesting point about this plot is that the seven objects that lie to the left of the $P_{\rm int}=2$ per cent line (dashed line), and have contrast below ∼0.3, are all objects with strong emission lines typical of Seyfert-type spectra (represented in the plot by names in brackets). Even though some Seyfert galaxies are known that have high linear polarizations (Brindle et al. 1990), it is clear that in the case of these radio-loud objects their polarizations are generally below 2 per cent. Furthermore, these polarizations are systematically lower than those of the other low break contrast sources.

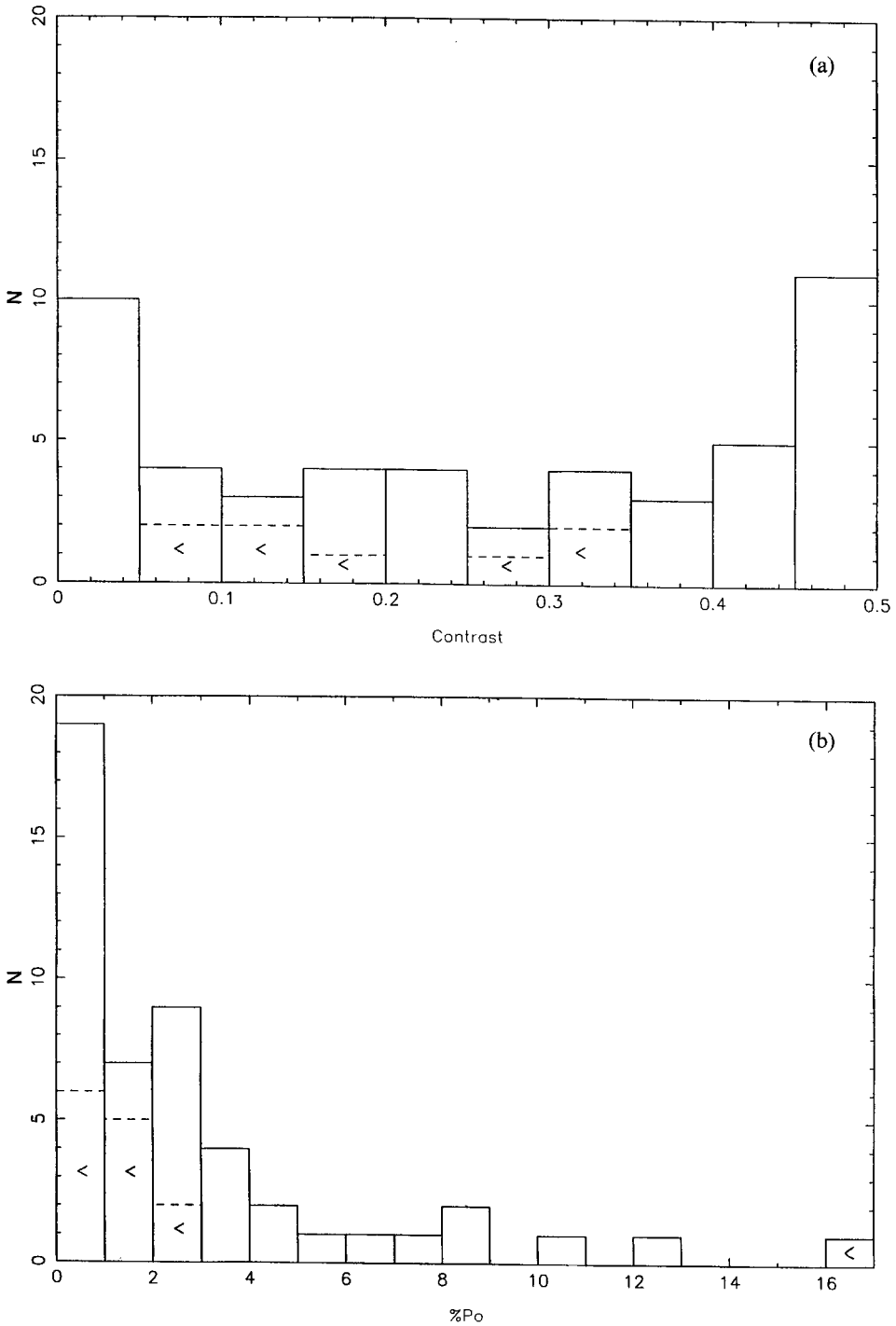

Figure 3. Distribution of break contrast as defined in the text (a), and percentage optical polarization (b) for the objects of the 200-mJy sample. Dashed bins with the < symbol correspond to upper limit values.

5.2 The distribution of emission-line EWs

We have argued that the emission-line EW can be used as a guide to the origin of the extra continuum inferred from break contrast or polarization measurements. In particular, strong emission lines are an indication of the presence of a Seyfert-type nucleus with its characteristic blue continuum emission, whereas the absence of strong lines is an indication that the galaxy contains a BL Lac nucleus. In Fig. 5 we show the distribution of EW for the strongest emission line for all the objects in the sample except those three sources for which we do not have spectroscopic information. It is clear from this distribution that most objects in the 200-mJy sample do not have strong lines. All objects, except the 10 sources with Seyfert-type spectra, have emission features with EW ≤ 60 Å.

It is important to note that this distribution corresponds to the EW of the strongest emission feature in the spectrum,

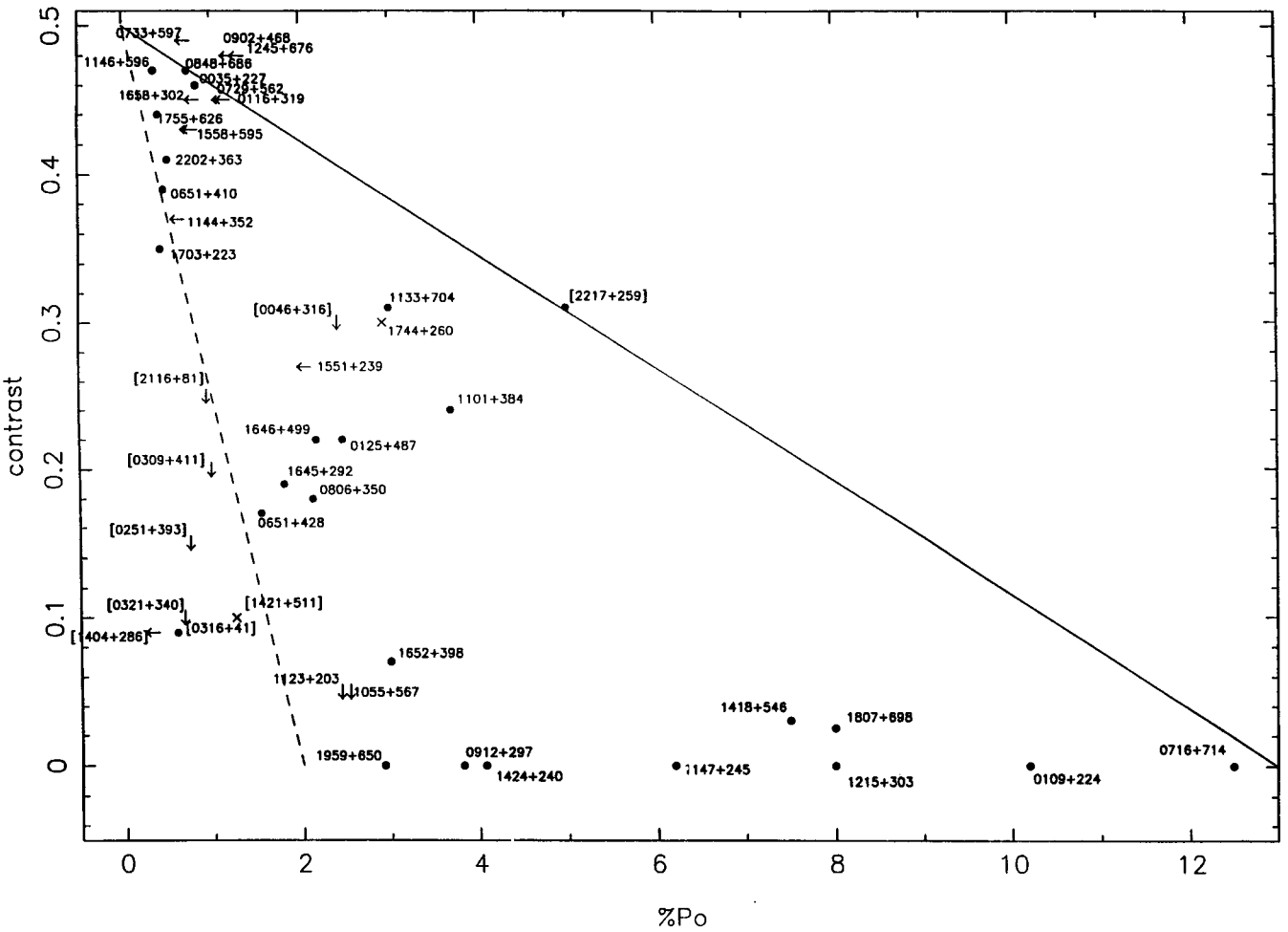

Figure 4. Break contrast versus percentage optical polarization for the 46 objects of the 200-mJy sample with the relevant data. The lines represent the expected variation of the observed polarization owing to the dilution of different amounts of starlight. The dashed line corresponds to an intrinsic polarization of 2 per cent and the solid line to a 13 per cent value. The sources whose names appear in brackets are those with a Seyfert-type spectrum. The arrows correspond to upper limit values and the crosses represent objects for which both values of contrast and optical polarization are upper limits.

hence not always the same emission line. In principle this could give rise to biases in the analysis since different emission lines are related to different physical processes in the source. However, this is not thought to introduce a major bias for two reasons. First, the vast majority of objects showed Hα + [N II] as their strongest line. Secondly, to bias the separation between BL Lacs from other types of objects, it would be necessary that the objects being classified as BL Lacs were those for which the strong emission line (for example Hα) was systematically outside the observational window, and also those for which the percentage optical polarization was systematically low. This is not the case for the objects that are classified as BL Lacs and BL Lac candidates in the present sample.

5.3 The contrast–EW distribution and the classification of BL Lac objects

Fig. 6 shows the break contrast–EW distribution for the 40 objects with available data and EW $\leq$ 60 Å. This distribution leaves out 10 objects with Seyfert-type spectra and emission lines with EW > 60 Å, three objects without spectra and two without published data on the 4000-Å break contrast.

First we compare this contrast–EW plot with the equivalent one published for the EMSS (see fig. 4 of Stocke et al. 1991). The major points to be noted are the following.

(i) Both distributions show a group of objects with break contrast $\leq$ 0.4 and with emission-line EWs extending up to values of 50 or 60 Å. In the case of the 200-mJy sample these objects are identified with galaxies (fuzz is evident from the POSS) and in the EMSS case the objects have been identified with either clusters of galaxies, or normal ellipticals (these having EW typically below 5 Å).

(ii) Both distributions have a significant number of objects at low contrast and small EW, although in the EMSS sample these objects seem to gather preferentially within the box limited by EW $\leq$ 5 Å and contrast $\leq$ 0.25, whereas in the 200-mJy sample the objects show a wider spread in both EW and break contrast values.

(iii) In both samples there are three objects that have

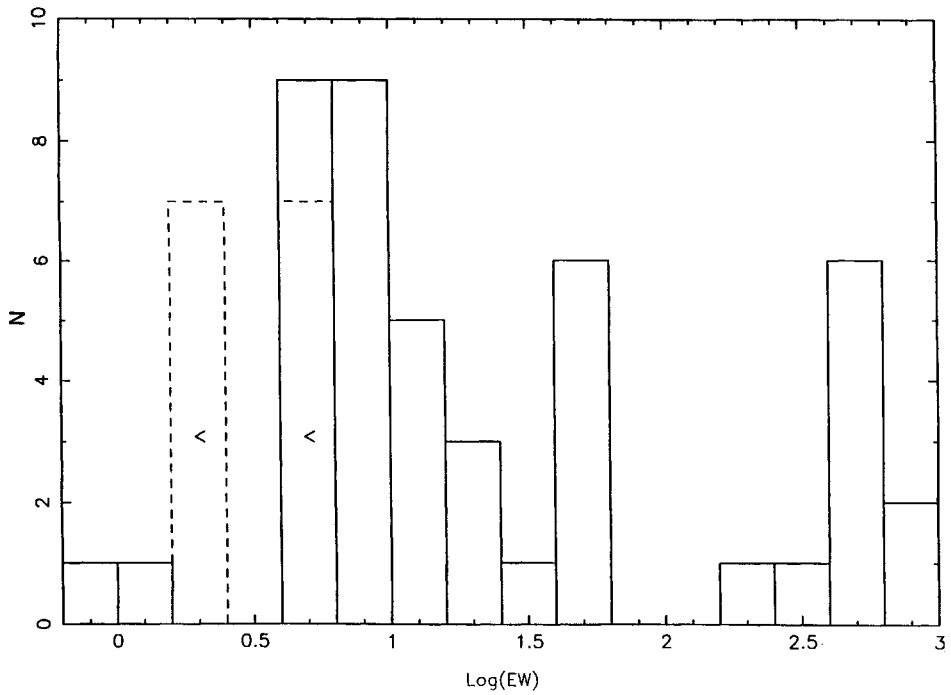

Figure 5. The distribution of EWs of the strongest emission feature in the spectra of the sources in the 200-mJy sample. Dashed bins with a < symbol represent upper limit values.

contrast below ~ 0.3 and EW between 40 and 60 Å, which in the case of the EMSS have been identified with clusters of galaxies.

(iv) In the EMSS there are several objects classified as 'weak-lined' AGN at zero contrast and with EW ranging from approximately 15 to 40 Å and for which there is no parallel in the 200-mJy sample.

In summary, apart from the finding of a few AGN with weak emission lines and very small contrast in the EMSS, the contrast–EW distributions for objects with EW ≤ 60 Å in the 200-mJy radio sample and the EMSS X-ray sample show the same type of objects. What we want to do next is to use the information on the contrast–EW plot to separate BL Lacs from other types of sources.

It is common practice to classify as BL Lacs those objects that have break contrast ≤ 0.25 and EW ≤ 5 Å (e.g. Stocke et al. 1991). We will examine whether these selection criteria can be improved upon. The first relevant fact is that, based on the results of Dressler & Shectman (1987), the objects with contrast ≤ 0.4 (and not just contrast ≤ 0.25) are likely to have an extra source of continuum (see Section 5).[1] The second is that contrast and emission-line EW will be correlated if the line luminosity is not dependent on the observed continuum strength, as one might expect in BL Lac objects where the non-thermal continuum is thought to be highly beamed and probably contributing little to the overall total of available ionizing photons.[2] Thus, changing the viewing angle and/or the luminosity of the BL Lac relative to that of the host galaxy will move an object on a slanting trajectory in the contrast–EW plane. We therefore think it preferable to discriminate between BL Lac objects and other AGN in terms of the emission-line luminosity relative to the galaxy starlight rather than relative to the total continuum emission as one does if one uses EW. We still, however, have to decide what a sensible dividing line luminosity might be.

As a starting point, we take the well-known BL Lac object 3C 371 (1807 + 698) and determine the EW of its strongest line relative to the starlight. We find that it must be ≥ 60 Å. In Fig. 6 we plot as a solid line the variation of EW with contrast for a galaxy ($C \sim 0.5$) with an emission line of EW = 60 Å. We suggest that objects similar to 3C 371 should still be classified as BL Lacs if viewed at an angle such that the continuum is less prominent relative to the starlight. Also, why should objects with intrinsic synchrotron luminosities a few times less than that of 3C 371 not be called BL Lacs? Hence, if we are looking for a region in the contrast–EW plane in which all objects should be classified as BL Lacs, instead of considering the rectangular region used by Stocke et al. (1991), we should take a triangular area limited by the lines of break contrast = 0.4 and a sloping line such as the one shown in Fig. 6. Of course this

[1]We, however, acknowledge that a change in the limiting contrast from 0.25 to 0.4 does not affect the BL Lac selection in the EMSS according to fig. 4 of Stocke et al. (1991).

[2]We do not speculate upon where the majority of ionizing photons might originate from but point out that the changes in the emission-line strengths in BL Lac (Vermeulen et al. 1995) and in 0521 − 365 (Scarpa, Falomo & Pian 1995) which seem to be uncorrelated with continuum changes suggest that such a source of photons does exist in BL Lacs.

dividing line is still to some extent arbitrary, but we adopt it because 3C 371 is widely accepted as a genuine BL Lac object and hence all objects found to the left of the line could be argued to be more BL Lac-like than 3C 371. We therefore propose that all the objects in Fig. 6 that have contrast ≤ 0.4 and which lie to the left of the full line should be considered as BL Lacs or BL Lac candidates, with the possible exception of 0651 + 410. The justification for classifying individual objects as BL Lacs and BL Lac candidates is given below.

0651 + 410 This source is a Zwicky elliptical galaxy and it is the only object with contrast < 0.4 that is to the left of the solid line and which we do not claim as a BL Lac or BL Lac candidate. The spectrum of this source shows Hα + [N II] emission with EW ~ 30 Å, although Merighi et al. (1991) report an EW of 4.7 Å for [N II] as the strongest emission in the spectrum they observed. This difference could be because of variability. The break contrast measured in the spectrum we obtained is 0.39, and its polarization measurements are well below the 2 per cent level. The properties of this source are so borderline that, even though this object could be a weak BL Lac diluted by the starlight of the host galaxy, it could just as well be a flat radio spectrum galaxy with a naturally low break contrast.

0651 + 428 The spectrum of this source showed Hα + [N II] emission with an estimated EW of 8 Å, a value not far from the 'traditional' 5-Å limit used for BL Lac classification, plus a break contrast of ~ 0.17 indicative of an extra source of continuum. Moreover, the source is polarized at ≥ 2 per cent which is well above the polarization measured for the reference stars (see Table 2). Hence, this source is a good BL Lac candidate.

0806 + 350 This source is a new BL Lac. Its spectrum showed only absorption features and the 400-Å break contrast is 0.18 which is indicative of an extra source of continuum. Furthermore, the optical polarization was measured above the 2 per cent level, and well above the level of polarization for the reference stars.

1055 + 567 This source turned out to be the one with the highest redshift ($z = 0.410$ measured from the [O III] λ4959 and 5007-Å emission feature). At this redshift, any possible Hα emission was too far into the red to fall in the observed spectral range. Hence, the EW is that of the [O III] λ5007 Å

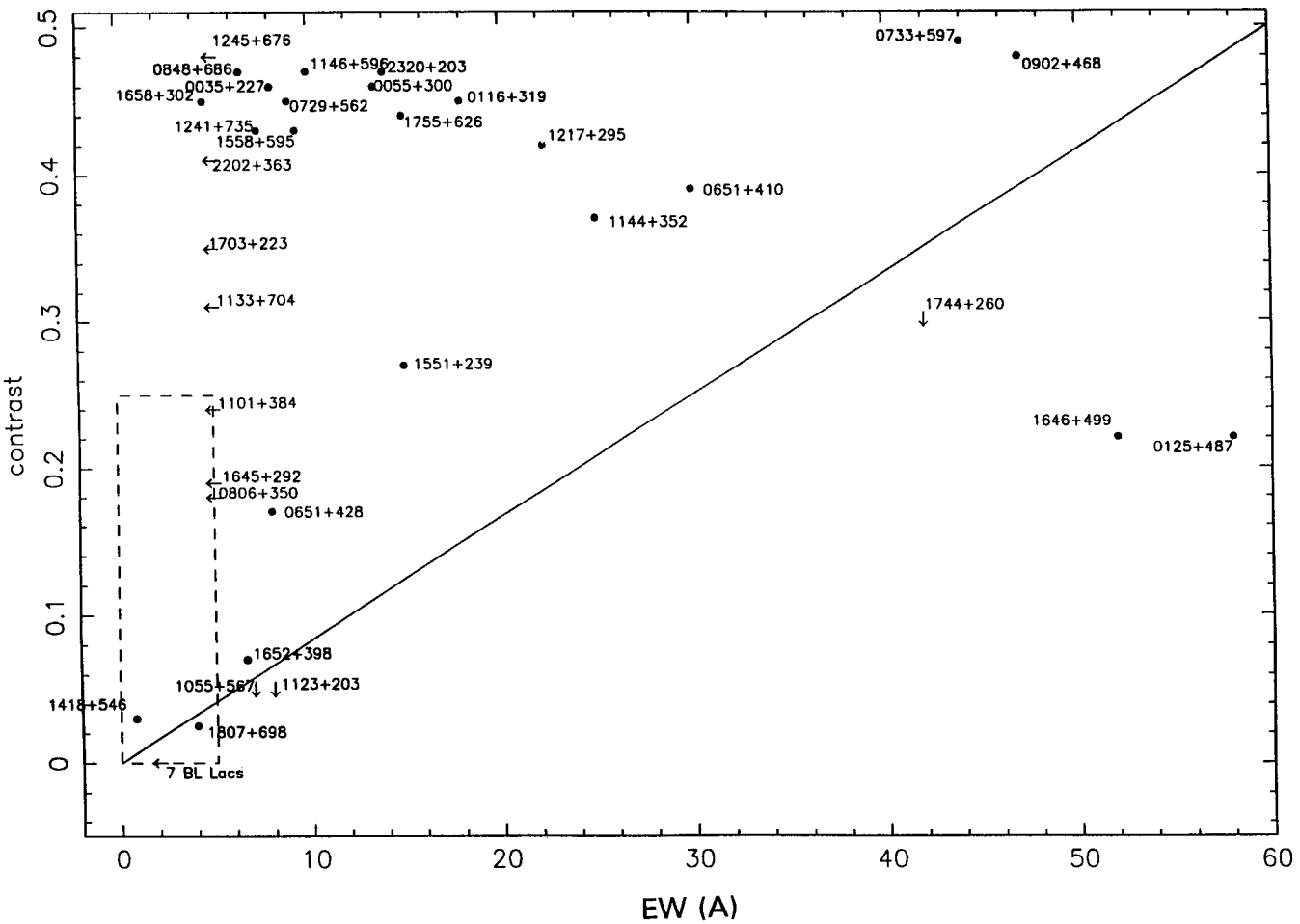

Figure 6. The contrast–EW plot representing the distribution of break contrast versus the EW of the strongest emission feature in the spectra of the sources of the 200-mJy sample. The distribution is only shown out to EW = 60 Å, thus leaving out the 10 objects with Seyfert-type spectra. The full line represents the expected decrease for the EW of an emission line in the presence of an increasing amount of continuum (see text for details). The area enclosed by the dashed line corresponds to EW ≤ 5 Å and contrast ≤ 0.25, as used by Stocke et al. (1991) for the classification of BL Lacs in the EMSS. Arrows correspond to upper limits.

and is estimated to be ~ 7 Å, a value very close to the 5-Å limit. The source also has a small estimated break contrast and was found to be polarized at the 2.5 per cent level, well above that of the reference stars. Although there is the possibility of stronger Hα emission existing, this source is considered a BL Lac candidate.

1123 + 203 The spectrum of this source shows [O II] λ3727-Å emission stronger than [O III] λ5007 Å, and, although it is possible to identify the Ca II H&K feature, the break contrast is estimated to be ~ 0.05. If there is Hα emission it will coincide with the edge of the observed spectral range and so the strongest EW was that of [O II] emission which slightly exceeds the 5-Å limit. However, the source was found to be polarized above the 2 per cent level, and well above the values found for the reference stars. The object is a good BL Lac candidate.

1144 + 352 This is an interesting object, especially because its radio polarization is 2.8 per cent at the 2σ level. Although we have not yet discussed radio polarization (this will be done in the next section), it is worth mentioning that such a high value is not common among the objects of the sample. We classify this object as a BL Lac candidate even though its spectrum shows Hα + [N II] emission with EW ~ 25 Å and a break contrast ~ 0.37. Both of these values are above the traditional limiting EW and contrast used by Stocke et al. (1991) for the classification of the EMSS BL Lacs. However, as we mentioned in the beginning of this section, contrast and EW are correlated, and, the higher the contrast, the larger the measured EW. Hence, this object could be a diluted BL Lac. Also, the fact that its measured optical polarization is below 2 per cent could arise from starlight dilution by the host galaxy.

1551 + 239 Among the BL Lac candidates, this object is probably the most marginal one, not only because the EW of its strongest emission line and break contrast exceed the limiting values used by Stocke et al. (1991), but also because of its lack of optical polarization. Nevertheless, because variability may play a role in decreasing the polarization, and because of the fact that the placement of the object in the contrast–EW plot is not very far from the other BL Lacs and BL Lac candidates, the source is maintained as a BL Lac candidate.

1645 + 292 This source is classified as a new BL Lac. As in 0806 + 350, the spectrum showed only absorption features and a low value for the break contrast. The optical polarization is close to the 2 per cent level and significantly above that of the reference stars. The source also has radio core polarization above 2 per cent.

1703 + 223 No emission features were identified for this source and any possible identification should have EW < 5 Å. The fact that its break contrast was found to be above the limiting value used by Stocke et al. (1991) is not regarded as a strong reason against a BL Lac classification. Although the optical polarization for this source is below the 2 per cent level, this object is classified as a BL Lac candidate.

Apart from the objects already discussed, we observed two extra sources, 0149 + 710 and 0210 + 515, that do not belong to the sample because their galactic latitude is below the required limit of $|b| < 12$, and therefore were not plotted on any of the plots. However, their estimated values of break contrast, EW, and percentage of optical polarization suggest that these objects are, respectively, a BL Lac candidate and a new BL Lac.

Finally, we comment on two of the three objects that lie to the right of the solid line in Fig. 6: 0125 + 487 and 1646 + 499. (In fact, there are 10 more objects that also lie to the right of this line but which are not represented on the plot; they are the objects with Seyfert-type spectra the emission lines of which have EW $\gg 60$ Å.) These three sources have enough extra continuum to produce a low break contrast as in a BL Lac or a Seyfert-type object, but their emission lines show EWs either too strong to be included in the first category, or rather weak to be included in the second. Of these three sources, the most intriguing one is 1646 + 499 because of its broad emission line and because the source showed polarization variability on consecutive days. This object appears to be a hybrid source which shows properties characteristic of BL Lacs, such as the variability of optical polarization, and of flat-spectrum radio quasars (FSRQs), such as the broad emission lines. What makes this source stand out from other FSRQs is that its 5-GHz luminosity of 1.6×10^{24} W Hz^{-1} puts it below the 10^{25} W Hz^{-1} limit at which quasars are usually considered radio-loud (Miller, Rawlings & Saunders 1993); what makes it stand out from most BL Lacs is its broad lines. Another peculiar object is 0125 + 487 which lies in the same region of the plot as the 1646 + 499 source. The two may be intrinsically similar objects. Given the recent discovery of a broad-line region (BLR) in BL Lac (Vermeulen et al. 1995), together with the BLR in 1646 + 499, this may indicate that BLRs are present in many BL Lac objects, although they are certainly difficult to see in most circumstances.

5.4 The percentage radio polarization

We now discuss those galaxies with break contrast > 0.4. The vast majority of them have EW ≤ 20 Å and so we consider the hypothesis that these sources may be little different from those objects that have break contrast below 0.4, except that their non-thermal continuum is weaker. In other words, we investigate the idea that they may host weak BL Lac-type nuclei. Can we test this idea? We follow up the suggestion by Gabuzda & Cawthorne (1993) that the percentages of radio core polarization for radio galaxies and BL Lacs are systematically different: the former they claim to be essentially unpolarized, and the latter to have polarization ~ 2 per cent. Their conclusion is based on very long baseline interferometry (VLBI) polarization measurements of a small sample. However, the 200-mJy sample is much larger and we can use available VLA radio polarization data to investigate the trend found by Gabuzda & Cawthorne (1993). If the radio core polarization is different in radio galaxies and the other objects, then the 200-mJy data should reflect this trend. For the purpose of comparison, the contrast data corresponding to the objects in the contrast–EW plot of Fig. 6 are plotted against the percentage of radio core polarization at 8.4 GHz (Akujor & Patnaik 1993; A. Patnaik, private communication) in Fig. 7 (once again, the arrows represent those objects that only have 2σ upper limits for the percentage polarization). Apart from the source 2320 + 203, all of the other galaxies that have contrast ≥ 0.4 show low levels of radio core polarization at

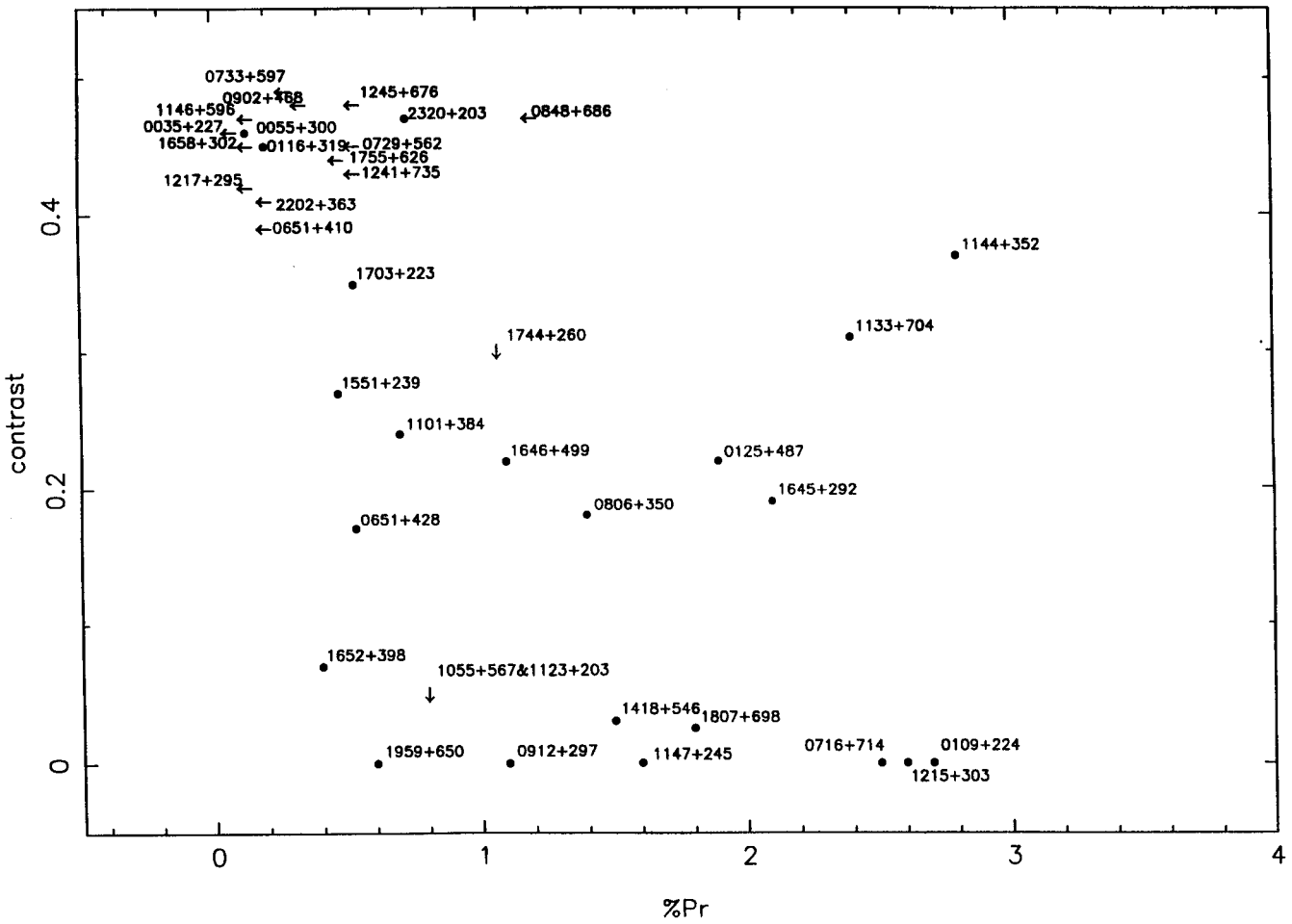

Figure 7. The distribution of contrast versus percentage of radio polarization at 8.4 GHz for the same objects as in the previous plot, i.e., those for which the strongest emission line had EW ≤ 60 Å. Arrows correspond to upper limit values.

8.4 GHz whereas many, but not all, BL Lacs have higher radio polarizations. Thus, the analysis of the 200-mJy sample supports the result suggested by Gabuzda & Cawthorne (1993), i.e., that radio galaxies with no evidence for optical continuum emission, other than from stars, have statistically different radio polarization properties from the known BL Lac objects, i.e., those that show evidence of another continuum emission component. This suggests that our hypothesis above is not correct and maybe not all the flat-spectrum objects identified with galaxies have BL Lac nuclei. However, it should be noted that the fact that a given source shows low levels of radio polarization does not necessarily exclude the possibility of it being a BL Lac since there are known BL Lacs with low radio core polarization (e.g. 1652 + 398).

5.5 Summary of the 200-mJy sample

The 200-mJy sample of flat radio spectrum sources contains 55 objects. We have obtained spectra for 46 objects, 24 of which did not possess previous spectral information. Redshifts are now known for 46 of the objects. In addition to these 46 sources there are seven with featureless spectra, two sources that were not observed spectroscopically (2214 + 201 and 2337 + 268), and another source (2319 + 317) for which a spectrum was obtained but in which no features were seen because of the poor S/N ratio. Since spectroscopic observations were taken for 46 out of the 55 objects it has been possible to carry out a self-consistent analysis of the spectra.

As far as BL Lac objects are concerned, the 200-mJy sample contains 13 previously known objects, two new BL Lacs, and six BL Lac candidates. The fraction of BL Lac objects is over 30 per cent in the 200-mJy sample which is similar to the values found for other radio-selected samples under the same circumstances. An extra new BL Lac (0210 + 515) and BL Lac candidate (0149 + 710) are reported here, although they are not part of the sample because their $|b| < 2$.

5.5.1 *The 'complete' sample*

The redshift distribution for the entire sample is shown in Fig. 8. The number of objects suffers a sharp cut-off at redshifts greater than 0.1 since the selection criteria specifically biased the sample towards low z. In fact, inspection of the Hubble relation for the data of the 3CR catalogue (Smith & Spinrad 1980) shows that a limiting

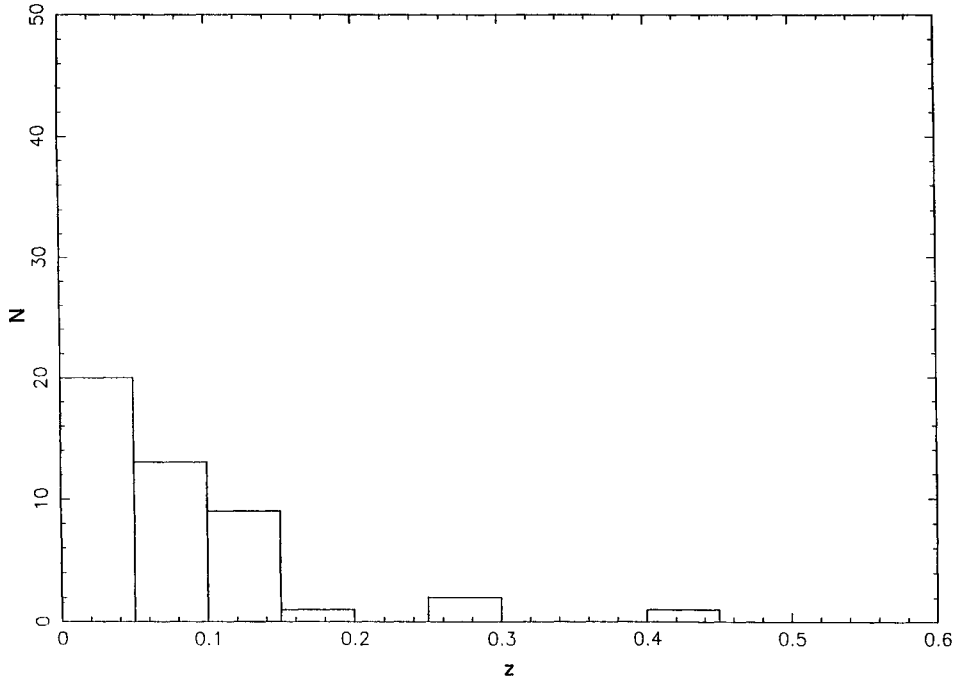

Figure 8. The redshift distribution for the 46 objects with known redshifts in the 200-mJy sample.

magnitude of $V=17$ corresponds to a redshift cut-off slightly above 0.1. The value of $\langle V/V_{max}\rangle$ for the objects with $z \leq 0.1$ is 0.50, thus indicating a uniform spatial distribution, and consistent with the sample being complete out to this redshift. The calculation of the local radio luminosity function for the flat radio spectrum sources, with a flux density limit of 200 mJy, is the topic of a forthcoming paper.

The 'complete' 200-mJy sample is defined as the subset of 40 objects that have $z \leq 0.1$, or which have featureless spectra. Of these seven BL Lacs with featureless spectra (hence no redshifts) only a small fraction are likely to turn out to have $z \leq 0.1$. The 33 objects with redshift measurements can be grouped into five categories:

(i) four previously known BL Lacs, one new BL Lac and three BL Lac candidates;
(ii) seven out of the 10 objects with Seyfert-type spectra;
(iii) 14 of the 17 galaxies with high contrast and EW ≤ 50 Å;
(iv) the peculiar objects 0125 + 487 and 1646 + 499;
(v) two objects with incomplete spectral information.

6 SUMMARY AND CONCLUSIONS

We have selected a radio and optical flux density limited radio sample of flat radio spectrum sources with three major aims in mind: to find new BL Lac objects with lower radio luminosity than the RBLs previously known; to investigate the observational boundaries between BL Lacs and other flat radio spectrum sources; and finally to create a sample of nearby objects, the host galaxies of which would be easy to study. Four parameters were used to analyse this sample: optical and radio polarization; the 4000-Å break contrast; and the EW of the strongest emission line. The availability of these four parameters allowed the identification of the following trends. The majority of the objects in the 200-mJy sample showed spectra with weak emission lines, although 10 sources showed Seyfert-type spectra. The 4000-Å break contrast distribution for the sample is bimodal with a group of objects preferentially showing values between 0 and 0.1 and another between 0.4 and 0.5. The distribution of optical polarization peaks at low values but it shows a long tail extending to higher values. Finally, the radio core polarization is systematically different for those sources with contrast below, and above, 0.4.

The information acquired on the four parameters mentioned above suggests that we separate the sources of the 200-mJy sample into two broad categories: those objects with break contrast <0.4 and those with break contrast >0.4. With the underlying assumption that the hosts of these objects are early-type galaxies, the results of the work by Dressler & Shectman (1987) show that those objects with break contrast values <0.4 have a very good chance of having an extra source of continuum. Hence, for these objects, the break contrast can be used as an indicator of the presence of emission in addition to the starlight of the galaxy. Among these objects we identify two new BL Lacs and six BL Lac candidates (plus a new BL Lac and BL Lac candidate which are not part of the sample owing to low $|b|$), a source with 'hybrid-type' properties between a BL Lac and a FSRQ, and another which may also show such characteristics, and finally sources with Seyfert-type spectra.

For the sources with contrast >0.4 it is not possible to use the break contrast as an indicator of the presence of an extra source of continuum. These are all identified with galaxies on the POSS plates, and we find that the vast majority of them have emission lines with EW ≤ 20 Å. The fact that the distribution of these objects according to contrast, EW and optical polarization seemed like a continua-

tion of the distribution observed for the other sources with weak emission lines but lower break contrast (the BL Lacs and BL Lac candidates) led us to hypothesize that these galaxies also hold BL Lac nuclei, only weaker. However, we find that the high-contrast galaxies have systematically lower radio core polarization than the BL Lacs and BL Lac candidates, thus suggesting some intrinsic difference. Although there are known BL Lacs that have low radio polarization, it is nevertheless interesting that such a systematic difference is observed. It suggests that not all the high-contrast flat radio spectrum galaxies hold BL Lac nuclei, something which is contrary to our initial hypothesis.

Finally, the conclusions of this paper are as follows.

(i) Combining observations of break contrast, percentage optical polarization and EW of emission lines can make a significant improvement in the process of identifying BL Lacs. We identify seven new BL Lac candidates in addition to three definite BL Lacs.

(ii) The lack of sharp separation between the objects with emission lines with EW ≤ 30 Å and break contrast below ~ 0.4 suggests that BL Lac objects can be identified within a wider range of values than those that have been used traditionally to classify this class of AGN.

(iii) The objects with Seyfert-type spectra showed preferentially weaker optical polarization values than the rest of the objects in the 200-mJy sample with break contrast < 0.4.

(iv) The existence of one, maybe two, sources that exhibit properties of both BL Lacs and FSRQs suggests that all BL Lac objects and FR1 radio galaxies may have BLRs. These BLRs must, though, be visible only under special conditions such as over a small range of viewing angles.

(v) We define a 200-mJy 'complete' sample which contains 33 objects with $z \leq 0.1$, plus seven featureless BL Lac objects without redshifts.

ACKNOWLEDGMENTS

MJMM acknowledges a Fellowship from PRAXIS-XXI (JNICT – Portugal) and PSS acknowledges support from NASA grant NAG 5-1630. We thank F. Owen for allowing us to use the spectral information on the source 0316 + 41 prior to publication, and P. Padovani for his helpful comments.

REFERENCES

Akujor C. E., Patnaik A. R., 1993, in Davis R. J., Booth R. S., eds, Sub-arcsecond Radio Astronomy. Cambridge Univ. Press, Cambridge, p. 277
Angel J. P. R., Stockman H. S., 1980, ARA&A, 8, 321
Armus L., Heckman T. H., Miley G. K., 1989, ApJ, 347, 727
Becker R. L., White R. L., Edwards A. L., 1991, ApJS, 75, 1
Blandford R. D., Rees M. J., 1978, in Wolfe A., ed., Pittsburgh Conference on BL Lac Objects. University of Pittsburgh Press, Pittsburgh, p. 328
Boksenberg A., Carswell R. F., Allen D. A., Fosbury R. A. E., Penston M. V., Sargent W. L. W., 1977, MNRAS, 178, 451
Brindle C., Baily J. A., Axon D. J., Ward M. J., Sparks W. B., McLean I. S., 1990, MNRAS, 244, 577
Browne I. W. A., Marchã M. J. M., 1993, MNRAS, 261, 795
Condon J. J., Broderick J. J., 1985, AJ, 90, 2540
Condon J. J., Broderick J. J., 1986, AJ, 91, 1051
Condon J. J., Broderick J. J., Seieslad G. A., 1989, AJ, 97, 1064
Dressler A., Shectman S., 1987, AJ, 94, 899
Filippenko A. V., Sargent W. L. W., 1985, ApJS, 57, 503
Gabuzda D. C., Cawthorne T. V., 1993, in Davis R. J., Booth R. S., eds, Sub-arcsecond Radio Astronomy. Cambridge Univ. Press, Cambridge, p. 211
Glenn J., Howell S. B., Schmidt G. D., Liebert J., Grauer A. D., Wagner R. M., 1994, ApJ, 424, 967
Heckman T. M., Black B., Crane P. C., 1980, A&AS, 40, 295
Impey C. D., Tapia S., 1990, ApJ, 354, 124
Impey C. D., Lawrence C. R., Tapia S., 1991, ApJ, 375, 46
Jannuzi B. T., Smith P. S., Elston R., 1993, ApJS, 85, 265
Kühr H., Schmidt G. D., 1990, AJ, 99, 1
Marchã M. J. M., Browne I. W. A., 1995, MNRAS, 275, 951
Marchã M. J. M., Browne I. W. A., 1996, MNRAS, 279, 72
Merighi R., Basso L., Vigotti M., Lahulla J. F., Lopez-Arroyo M., 1991, A&AS, 89, 225
Miller P., Rawlings S., Saunders R., 1993 MNRAS, 263, 425
Morris S. L., Stocke J., Gioia I. M., Schild R. E., Wolter A., Maccacaro M., Ceca R. D., 1991, ApJ, 380, 49
Patnaik A. R., Browne I. W. A., Wilkinson P. N., Wrobel J. M., 1992, MNRAS, 254, 655
Scarpa R., Falomo R., Pian E., 1995, A&A, 303, 730
Schachter J. F. et al., 1993, ApJ, 412, 541
Schmidt G. D., Elston R., Lupie O. L., 1992, AJ, 104, 1563
Schmidt M., Weynmann R. J., Foltz C. B., 1989, PASP, 101, 713
Shields G. A., Oke J. B., 1975, PASP, 87, 879
Sitko M. L., Schmidt G. D., Stein W., 1985, ApJS, 59, 323
Smith H. E., Spinrad H., 1980, PASP, 82, 553
Smith P. S., Hall P. B., Allen R. G., Sitko M. L., 1992, ApJ, 400, 115
Sparks W. B., Hough J. H., Axon D. J., Bailey J., 1986, MNRAS, 218, 429
Stickel M., Padovani P., Urry C. M., Fried J. W., Kühr H., 1991, ApJ, 374, 431
Stickel M., Kühr H., Fried J. W., 1993, A&AS, 97, 483
Stocke J. T., Morris S. L., Gioia I., Maccacaro T., Schild R. E., Wolter A., 1990, ApJ, 384, 141
Stocke J. T., Morris S. L., Gioia I., Maccacaro T., Schild R. E., Wolter A., Fleming T. A., Henry J. P., 1991, ApJS, 76, 813
Ulrich M.-H., 1978, ApJ, 222, L3
Vermeulen R. C., Ogle P. M., Tran H., Browne I. W. B., Cohen M. H., Readhead A. C. S., Taylor G. B., 1995, ApJ, 452, L5
Véron P., 1978, Nat, 272, 430
Véron-Cetty M.-P., Véron P., 1991, ESO Scientific Report, 10
Weistrop D., Shafer D. B., Hintzen P., Romanishin W., 1985, ApJ, 292, 614
White R. L., Becker R. H., 1992, ApJS, 79, 331
Wills B. J., Wills D., Breger Antonucci R. R. J., Barvainis R., 1992, ApJ, 398, 454
Wills D., Wills B. J., Breger M., Hsu J.-C., 1980, AJ, 85, 1555